Applied Soft Computing Journal 89 (2020) 106141

Contents lists available at ScienceDirect

Applied Soft Computing Journal

journal homepage: www.elsevier.com/locate/asoc

Constrained design optimization of selected mechanical system components using Rao algorithms

R.V. Rao *, R.B. Pawar

Mechanical Engineering Department, S. V. National Institute of Technolog, Surat, Gujarat 395007, India

ARTICLE INFO

Article history:
Received 23 September 2019
Received in revised form 22 December 2019
Accepted 27 January 2020
Available online 30 January 2020

Keywords:
Constrained design optimization
Mechanical components
Rao algorithms

ABSTRACT

The design optimization of mechanical system components, like bearings, pulleys, springs, etc. is an essential issue due to the current competitive market. The performance of any mechanical system depends on the design of their mechanical components. The design optimization of these mechanical components is a difficult task due to the intricate design constraints and mixed type design variables (i.e., continuous, discrete, and integer). This paper explores the performance of Rao algorithms on the design optimization of selected mechanical system components. The designs obtained using Rao algorithms are compared with the designs obtained using other optimization algorithms in previous studies. The comparison of results shows the ability and the efficiency of Rao algorithms for solving complex design optimization problems of mechanical components.

1. Introduction

Every machine assembles the number of mechanical components to get the desired outcome. The performance of any machine depends on the performance of its components. In today's competitive market, there is a high demand for cost-effective products. At the same time, the designed product should attain its safety regulations also. The cost of the product increases with the safety parameters of the product. Hence there is a need to develop the products which shall satisfy the minimum safety criteria at a low cost. To get the optimum design of any machine, the design optimization of its mechanical components becomes a vital task for designers. The design of mechanical components includes complex objective functions with a large number of mixed type design variables. Also, the design of these components is required to satisfy various design constraints for proper functioning.

The design optimization of mechanical components is a tedious process due to its complex formulations. The researchers have been working on design optimization of various mechanical components using different optimization algorithms. Some of the recently presented studies of design optimization are discussed here in brief. Baykasoğlu and Ozsoydan [1] proposed the adaptive firefly algorithm and used this algorithm to solve various mechanical design optimization problems such as a tension/compression spring, a pressure vessel, a welded beam, and a speed reducer. Cao et al. [2] performed design optimization of a gear blank preform which was based on the regression-constrained Gaussian process latent variables model (R-GPLVM) using genetic algorithm-extreme learning model (GA-ELM). Panda et al. [3] presented design optimization of a rolling element bearing using the PSO algorithm and a hybrid PSO–TLBO algorithm to enhance the fatigue life the bearing. Wang et al. [4] optimized the cycloid speed reducer using GA considering the volume and the efficiency as objectives. Kim et al. [5] performed the optimization of an angular contact ball bearing design for the main shaft of the grinder using a hybrid method employing both a regression-based sequential approximate optimizer and micro-genetic algorithm. Shinde and Pawar [6] carried out a multi-objective surface texturing optimization of a journal bearing for performance characteristics using grey relational analysis method.

Ding and Tang [7] presented a multi-objective optimization of machine-tool settings for hypoid gears by considering both physical and geometric performances. Gropper et al. [8] showed the optimization of surface textures for a tilting pad thrust bearing using an interior-point algorithm. Zhang et al. [9] studied design optimization of a planetary gear reducer using a genetic algorithm (GA) for load sharing performance and volume optimization. Rai et al. [10] presented optimization of helical gear design with a profile shift for reducing the volume of gear using a real coded genetic algorithm (RCGA). Miler et al. [11] studied design optimization of spur gear pair using GA to minimize the transmission volume and the power losses. Robison and Vacca [12] presented multi-objective optimization of a gerotor with circular teeth using non-dominated sorting genetic algorithm II (NSGA-II) for kinematics and wear.

* Corresponding author.
E-mail address: ravipudirao@gmail.com (R.V. Rao).

https://doi.org/10.1016/j.asoc.2020.106141
1568-4946/

Alessio [13] proposed a methodology for multi-objective optimization of gear design. The author had obtained Pareto-optimal solutions using a deterministic multi-objective optimization method combined with a direct-search global optimization algorithm. Tian and Lee [14] presented an aerodynamic shape design optimization using an improved fruit fly optimization algorithm. Hou et al. [15] showed a design optimization of hat-shaped composite T-joints in automobiles using NSGA-II. The authors had concluded that the mechanical properties of an optimized T-joint were enhanced effectively. Zhang et al. [16] proposed a hybrid teaching–learning-based optimization (TLBO) and neural network algorithm (NNA), which assembled the fast convergence rate of TLBO and the excellent global optimization ability of NNA. The authors had used this hybrid algorithm to optimize engineering design problems such as a welded beam, a tension/compression spring, a pressure vessel, and a speed reducer. Cheng et al. [17] solved the deconvolution problem for the fault diagnosis of a rolling element bearing using the PSO algorithm. Jat and Tiwari [18] used elitist NSGA-II for the optimization problem of a spherical roller bearing considering two objectives with eight design variables and twenty-two constraints.

From the literature study, it is observed that the researchers had used various advanced optimization algorithms that require the population size and the number of iterations as common controlling parameters. Besides, most of the optimizations algorithms also depend on their algorithm-specific control parameters, for example, GA depends on the mutation probability, the selection operator, and the crossover probability; ABC algorithm relies on the number of onlooker bees, scout bees, employed bees, and limit; PSO algorithm depends on its inertia weight, social parameter, and cognitive parameter. The performance of these optimization algorithms gets affected adversely due to improper tuning of the algorithm-specific parameters. The precise adjustment of the algorithm-specific control parameters is a tedious process which increases the computational efforts. Also, the working process of these advanced optimization algorithms is complex and challenging to understand for amateur designers and researchers. Due to these reasons, there is a need for the development of new optimization algorithms that are simple to understand and independent of algorithm-specific parameters.

Keeping the above points in view, Rao [19] proposed three algorithms which are simple, algorithm-specific parameter-less and metaphor-less optimization algorithms. The main advantage of Rao algorithms is that they do not require tuning of the algorithm-specific parameters to search the optimum solution of optimization problems. Also, the working procedure of Rao algorithms is quite simple, easy to understand, easy to implement, and straight forward. Hence, researchers and designers from different streams of science and engineering can apply Rao algorithms to solve optimization problems of real systems of their streams. Wang et al. [20] recently used the Rao-1 algorithm successfully to estimate model parameters of an actual commercial Photovoltaic cell. In this work, the performance of three Rao algorithms is explored on complex design optimization problems of selected mechanical system components such as a helical compression spring, a hydrostatic thrust bearing, a multiple disc clutch brake, a cylindrical roller bearing, a spherical roller bearing, a plate fin heat exchanger, a shell and tube heat exchanger, a welded beam, a belt–pulley drive, and a hollow shaft. Also, the convergence speed of Rao algorithms is showed in this paper using convergence plots of problems considered. For validation purpose, the results obtained using proposed Rao algorithms are compared with the results obtained using other different advanced optimization algorithms in previous studies, such as GA, PSO, artificial bee colony (ABC) algorithm, differential evolution (DE), genetic adaptive search (GeneAS), firefly algorithm (FA), branch and bound (B&B) method, hybrid swarm intelligence approach (HSIA), meta-genetic algorithm (MGA), GA aided stochastic optimization (GASO), hybrid ABC and grid search method (GSM), binary GA (GA), Bees algorithm (BA), imperialist competitive algorithm (ICA), falcon optimization algorithm (FOA), and biogeography-based optimization (BBO) algorithm.

The rest of the paper is structured as: Section 2 presents brief description of the proposed Rao algorithms, Section 3 presents description of the considered design optimization problems of the mechanical system components, Section 4 presents the results of computational experiments obtained using Rao algorithms for the selected optimization problems and their comparisons with the results of other optimization algorithms, and finally, Section 5 concludes the outcomes of this study.

2. Rao algorithms

The path of searching an optimal solution using Rao algorithms depends on the best and worst candidate solutions within the entire population and the random interactions between the candidate solutions. Let f is the fitness function which is to be maximized (or minimized). At any iteration w, assume that there are 'n' number of populations (i.e., candidate solutions, $u = 1, 2, \ldots, n$) and 'd' number of design variables. Let the best value of f (i.e., f_{best}) obtains with the best candidate variables i.e. *best* within the entire candidate solutions, and the worst value of f (i.e., f_{worst}) achieves with the worst candidate solution i.e. *worst* within the whole population. If $X_{u,v,w}$ is the value of the uth variable for the uth candidate during the wth iteration, then this value is updated using any one of the following three equations.

$$X'_{u,v,w} = X_{u,v,w} + r_{1,u,v,w}(X_{best,v,w} - X_{worst,v,w}), \tag{1}$$

$$X'_{u,v,w} = X_{u,v,w} + r_{1,u,v,w}(X_{best,v,w} - X_{worst,v,w}) + r_{2,u,v,w}(|X_{u,v,w} \text{ or } X_{U,v,w}| - |X_{U,v,w} \text{ or } X_{u,v,w}|), \tag{2}$$

$$X'_{u,v,w} = X_{u,v,w} + r_{1,u,v,w}(X_{best,v,w} - |X_{worst,v,w}|) + r_{2,u,v,w}(|X_{u,v,w} \text{ or } X_{U,v,w}| - (X_{U,v,w} \text{ or } X_{u,v,w})), \tag{3}$$

where, $X_{best,v,w}$ is the value of the best candidate for the variable v and $X_{worst,v,w}$ is the value of the worst candidate for the variable v during the wth iteration. $X'_{u,v,w}$ is the updated value of $X_{u,v,w}$ and $r_{1,u,v,w}$ and $r_{2,u,v,w}$ are the two random numbers for the uth candidate of vth variable during the wth iteration in the range [0, 1].

In Eqs. (2) and (3), the term $X_{u,v,w}$ or $X_{U,v,w}$ indicates that the uth candidate solution is compared with any randomly picked Uth candidate solution, and the information is exchanged based on their fitness function values. If the fitness function value of an uth candidate solution is better than the fitness function value of Uth candidate solution then the term "$X_{u,v,w}$ or $X_{U,v,w}$" becomes $X_{u,v,w}$ and the term "$X_{U,v,w}$ or $X_{u,v,w}$" becomes $X_{U,v,w}$. On the other hand, if the fitness function value of Uth candidate solution is better than the fitness function value of uth candidate solution then the term "$X_{u,v,w}$ or $X_{U,v,w}$" becomes $X_{U,v,w}$ and the term "$X_{U,v,w}$ or $X_{u,v,w}$" becomes $X_{u,v,w}$.

The searching process of global optimum is carried out using Eqs. (1)–(3) in Rao-1 algorithm, Rao-2 algorithm and Rao-3 algorithm respectively. Eqs. (1)–(3) can be expressed in simplified form as,

$$x_{new} = x_{old} + r_1(x_{best} - x_{worst}) \tag{4}$$

$$x_{new} = x_{old} + r_1(x_{best} - x_{worst}) + r_2(|x_{old} \text{ or } x_{random}| - |x_{random} \text{ or } x_{old}|), \tag{5}$$

$$x_{new} = x_{old} + r_1(x_{best} - |x_{worst}|) + r_2(|x_{old} \text{ or } x_{random}| - (x_{random} \text{ or } x_{old})) \tag{6}$$

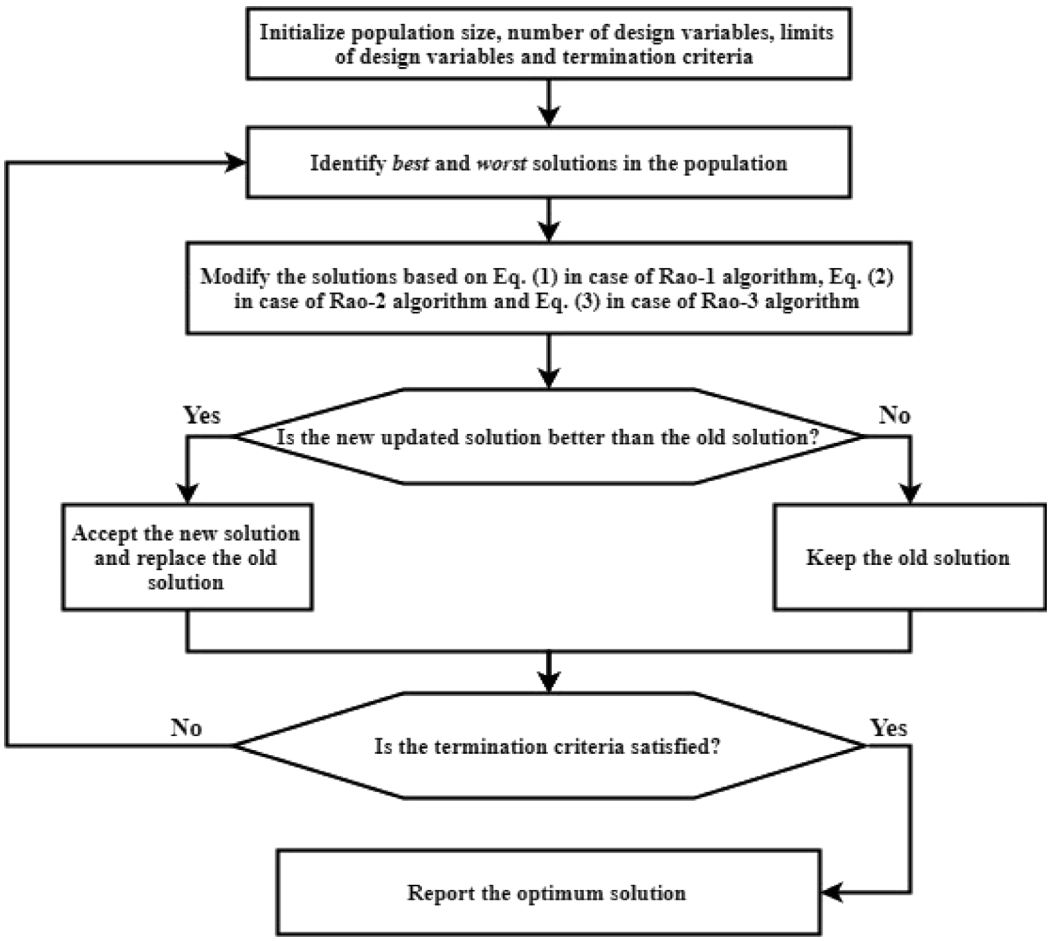

Fig. 1. Flowchart of the Rao algorithms.

In Eqs. (4)–(6), x_{new} means newly updated candidate solution for a variable, and x_{old} means old candidate solution of the variable. Just like the TLBO algorithm [21] and Jaya algorithm [22–24], these three Rao algorithms are also independent of algorithm-specific parameters, and thus the efforts of designers are reduced to tune the precise algorithm-specific parameters for obtaining the best results. Fig. 1 illustrates the flowchart of Rao algorithms. This flowchart shows the simplicity of Rao algorithms than other optimization algorithms. The MATLAB codes of these three Rao algorithms have been given by Rao [19] considering a benchmark *sphere function*.

The Rao algorithms move the population in the search space on the basis of interactions made by the population with the best, worst, and randomly selected solutions. The preliminary experiments conducted on the constrained and unconstrained optimization benchmark problems [19] revealed the effectiveness of these algorithms. Furthermore, from the preliminary computational experiments presented in Rao [19], it can be observed that the three Rao algorithms are performing well and competitive with each other. These algorithms were tested using 25 optimization benchmark problems having characteristics such as unimodality, multimodality, separability, non-separability. The individual performance of each Rao algorithm is better than those of the remaining two algorithms in different problems. For 20 problems, the Rao-1 algorithm's performance (mean values) is better or equal to that of the Rao-2 and Rao-3 algorithms; for 17 problems, Rao-2 algorithm's performance is better or equal to the performances of the remaining two algorithms; and for 20 problems, Rao-3 algorithm's performance is better or equal to that of the remaining two algorithms. This indicates that these algorithms have different characteristics in exploring and exploitation of the search process.

The general framework of the Rao-1 algorithm is described in Algorithm 1. The Frameworks of the Rao-2 and Rao-3 algorithms are similar to the framework presented in Algorithm 1, except that the Eq. (1) will be replaced by the respective algorithms' equations.

3. Description of the considered optimization problems

In this section, ten design optimization problems of mechanical components, such as a helical compression spring, a hydrostatic thrust bearing, a multiple disc clutch brake, a cylindrical roller bearing, a spherical roller bearing, a plate fin heat exchanger, a shell and tube heat exchanger, a welded beam, a belt–pulley drive, and a hollow shaft are described briefly. The design formulations related to these ten optimization problems are given in the Appendix.

3.1. Helical compression spring

Fig. 2 shows the schematic diagram of a helical compression spring. The objective of this problem is the minimization of the volume of the spring. This problem consists of three mixed type design variables such as, the diameter of winding coil (D), the wire diameter (d), and the number of coils (n). Here, D is a continuous variable, d is a discrete variable, and n is a integer variable. There are eight design constraints that are related to the

Algorithm 1: *framework of the Rao-1 algorithm*

BEGIN

Initialize 'n'- number of solutions, 'd'- number of design variables, 'LB'- lower boundaries of design variables, 'UB'- upper boundaries of design variables, and 'FE_max'- termination criterion;

Generate the initial candidate solutions and find fitness values (f), function evaluations counter = $FE = 0$, iteration counter = $w = 0$;

While $FE < FE\_Max$

$w = w + 1;$

$FE = FE + n;$

Identify the best ($X_{best,v,w}$) and worst ($X_{worst,v,w}$) solutions based on the fitness values

For u=1→n

For v= 1→d

$X'_{u,v,w}$ → Update the variables of $X_{u,v,w}$ candidate solution using Eq. (1)

$X'_{u,v,w} = X_{u,v,w} + r_{1,u,v,w}(X_{best,v,w} - X_{worst,v,w})$

$X'_{u,v,w}$ → Check the boundary condition violations and apply the bound values in case of violations

End For

End For

f'- Evaluate the fitness values for the updated solutions

For u=1→n

If $f'(u)$ better than $f(u)$

$$f(u) = f'(u)$$

End If

End For

End While

Report the final solutions

END

shear stress, the wire diameter, the outer diameter of the coil, the ratio of the inner coil diameter to the wire diameter, and the deflection of the spring. This problem was previously attempted by [25–29].

3.2. Hydrostatic thrust bearing

Fig. 3 shows the schematic diagram of a hydrostatic thrust bearing. The objective of this problem is to minimize the power loss during the working of the bearing. This problem consists of four design variables such as radius of bearing step (R), recess radius (R_o), viscosity of oil (μ), and the flow rate of oil (Q). There are seven non-linear inequality design constraints which are related to the inlet oil pressure, load carrying capacity, thickness of oil film, oil temperature rise, and the geometrical constraints. This problem was previously attempted by [21,24,26].

3.3. Multiple disc clutch brake

Fig. 4 shows the schematic diagram of a multiple disc clutch brake. The objective of this problem is the minimization of the total mass of the clutch brake while satisfying eight non-linear constraints. This problem consists of five discrete design variables namely, the outer radius (r_o), inner radius (r_i), disc thickness (t), actuating force (F), and the number of contact surfaces (Z). This problem was previously attempted by [21,24,30].

3.4. Cylindrical roller bearing (CRB)

Fig. 5 shows the schematic diagram of a CRB. Roller bearings are preferred generally in heavy load and medium speed applications, such as crane hooks, cone crushers, pulverizers, etc., due to their higher load-carrying capacity than ball bearings. The bearing life corresponds to its fatigue life and depends upon the dynamic load capacity (C_d). Hence, to maximize the bearing life, the C_d is to be maximized. Therefore, the maximization of

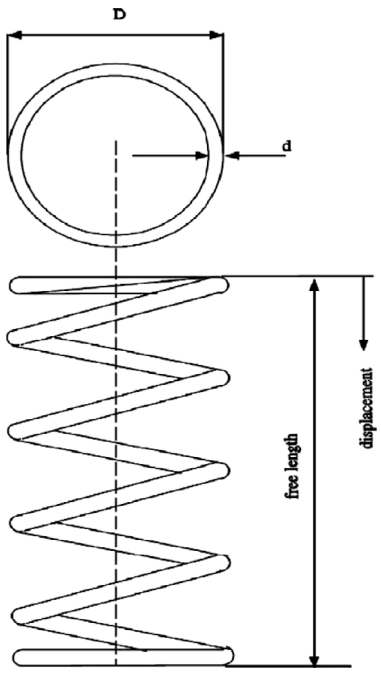

Fig. 2. Schematic diagram of a helical compression spring [28].

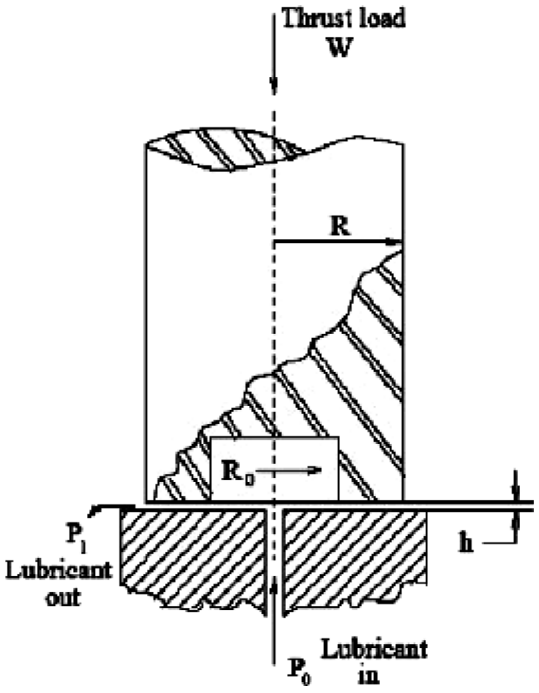

Fig. 3. Schematic diagram of a hydrostatic thrust bearing [21].

dynamic load capacity of the CRB is taken as an objective function. It consists of nine design variables out of which first four design variables come from inner dimensions of CRB, while other five are used as constraint variables. Parameters K_{Dmin} and K_{Dmax} decide the feasible range of the roller diameter (D_r), the value of e ensures the running mobility of bearing, the value of ε limits the thickness of bearing ring at the outer raceway, and the value of β limits the roller effective length (l_e). In this problem, nineteen constraints are considered based on the bearing running considerations, manufacturing, its internal geometries, and contact stresses [31,32].

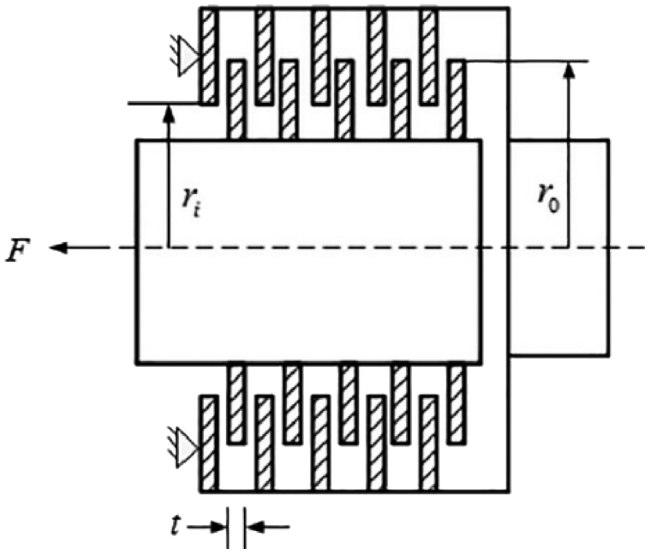

Fig. 4. Schematic diagram of a multiple disc clutch brake [21].

3.5. Spherical roller bearing (SRB)

The SRB geometry is complex and unique. Fig. 6 shows the schematic diagram of the SRB. The outer ring of the SRB has spherical shape at inner side. These bearings are self-aligning and can adapt the static as well as the dynamic misalignment. These bearings support both axial and radial loadings. SRBs are used in various applications such as, printing machines, rolling mills, crushers, construction machinery, papermaking machines, and vibrating screens. The detailed description and design analysis of the considered spherical roller bearing was presented by Jat and Tiwari [18]. In this problem, the maximization of dynamic load capacity of the SRB has been taken as an objective function which consists of eight design variables along with twenty-two design constraints.

3.6. Plate fin heat exchanger (PFHE)

Fig. 7 shows the schematic diagram of the PFHE. The objective of this problem is to minimize entropy generation units while satisfying twenty-two design constraints. This problem consists of seven design variables, such as the heat exchanger length for hot and cold fluids (L_h and L_c), the height of fin (H), the fin frequency (n), the fin thickness (t), the lance length of the fin (l), and the number of fin layers for the hot fluid (N_h). This problem was previously attempted by [33–36].

3.7. Shell and tube heat exchanger (STHE)

Fig. 8 shows the schematic diagram of the STHE. The heat exchanger with two tube passages and one shell passage for distilled water and raw water with 0.46 MW heat duty has to be designed for minimum total cost. This problem consists of three design variables such as, the tube outside diameter (d_o), shell internal diameter (D_s), and the baffles spacing (B) with eight design constraints related to the ratio of tube length to shell diameter, the tube side fluid velocity, the shell side fluid velocity, and the pressure drop of both tube and shell side. This problem was previously attempted by [36–41].

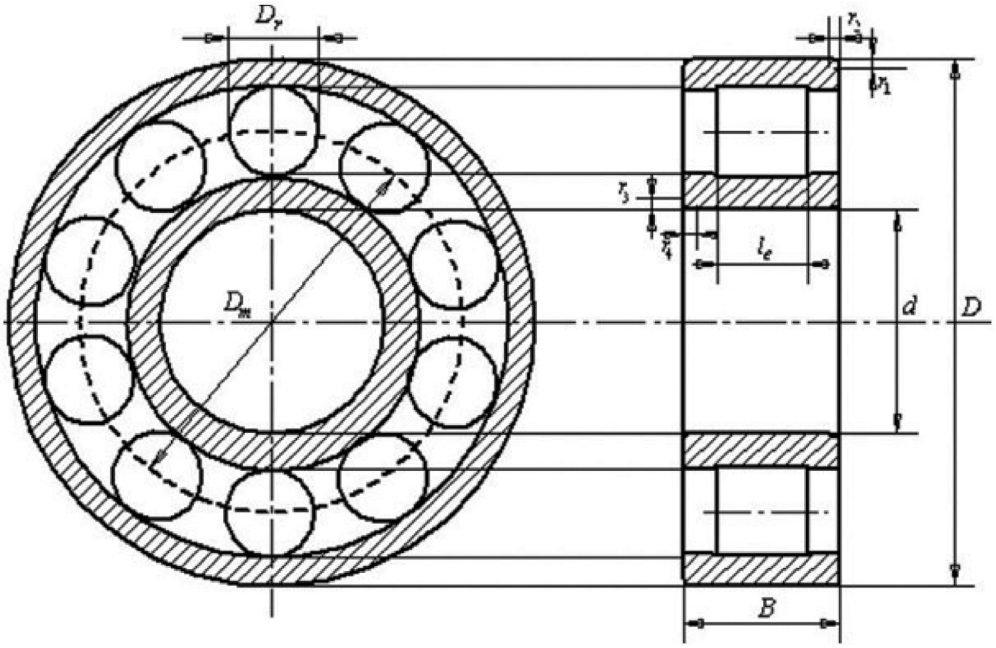

Fig. 5. Schematic diagram of a cylindrical roller bearing [31].

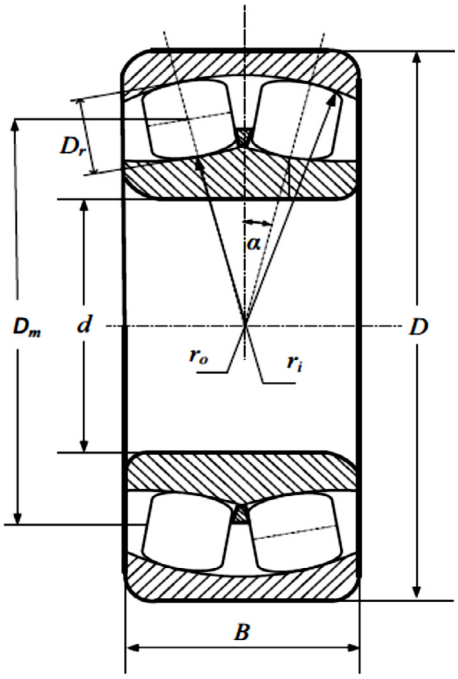

Fig. 6. Schematic diagram of a spherical roller bearing [18].

3.8. Welded beam

Fig. 9 shows the schematic diagram of the welded beam. The objective of this problem is the minimization of the overall fabrication cost while satisfying four design constraints. This problem consists of six variables out of which two are decision variables related to the welding choice and beam material, and other four are design variables such as the weld thickness (h), weld length (l), beam width (t), and the beam thickness (b). Here, h, t, and b are in integer multiples of 0.0625 in. and l is a continuous variable. In this problem, the coded values are assigned to the welding type choice (x_1) such as 0 for two-sided welding and 1 for four sided welding. Also, the coded values are assigned for beam material choice (x_2) such as 1 for Steel, 2 for Cast Iron, 3 for Aluminium, and 4 for Brass. This problem was previously attempted by [42–44].

3.9. Belt–pulley drive

Fig. 10 shows the schematic diagram of a belt–pulley drive. The objective of this problem is to minimize the total weight of pulleys which are to be used to transmit 10 HP power from one shaft to the another shaft by means of belts [45]. This problem consists of two design constraints with three design variables such as the diameter of pulleys (d_1 and d_2) and the width of pulleys (b).

3.10. Hollow shaft

Fig. 11 shows the schematic diagram of a hollow shaft. The objective of this problem is to minimize the weight of the hollow shaft which is to be used to transmit power from one point to the another by means of belt drive or gear drive [45]. This problems consists of two design variables such as the outside diameter of shaft (d_o) and the ratio of the inner diameter to the outer diameter of the hollow shaft (k). The design constraints are related to the torsional rigidity of the shaft and the buckling load carried by the shaft.

The next section presents the results of computational experiments for the considered design optimization problems obtained using Rao algorithms and also shows the comparison of these results with the results obtained for the same problems using other optimization algorithms in previous studies.

4. Computational results and discussion

The computational experiments are performed using the R2016b version of the MATLAB tool. A Laptop with a 1.90-GHz Intel Core i3-4030U processor and 8GB RAM is used for computational experiments. Rao algorithms are executed 30 times for each problem. The optimal designs obtained using each Rao

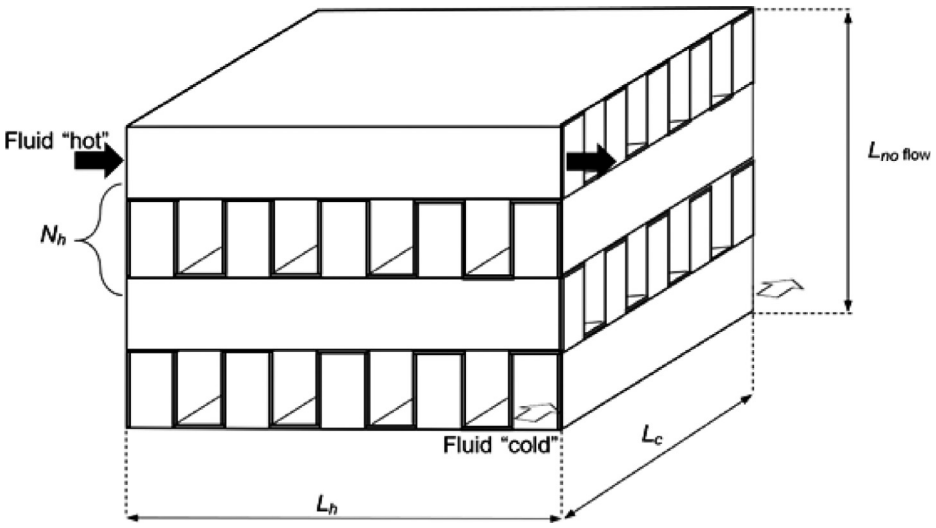

Fig. 7. Schematic diagram of a plate-fin heat exchanger [36].

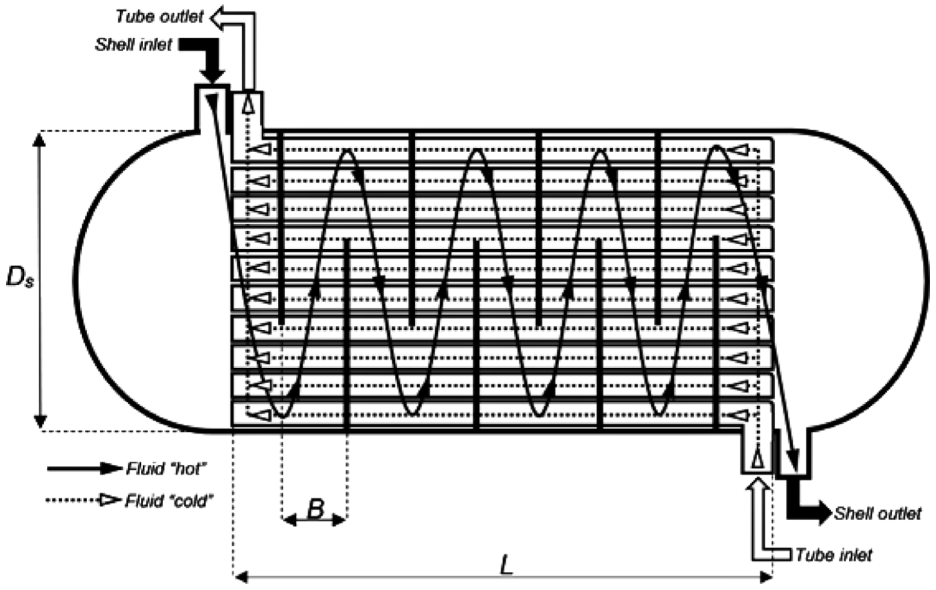

Fig. 8. Schematic diagram of a shell and tube heat exchanger [36].

algorithm are tabulated separately. The optimal designs and statistical results are compared with the same obtained using other optimization algorithms in previous studies. The results of the Jaya algorithm are also obtained in each problem for comparison except the multiple disc clutch brake problem and hydrodynamic thrust bearing problem as they are available in previous studies. For fair comparison with the results of other algorithms, the number of maximum function evaluations are kept same for Jaya and Rao algorithms. The precision of results up to six decimal points is considered in all problems.

In the case of helical spring design problem, the population size and the maximum number of function evaluations are considered as 40 and 75 000 respectively in each Rao algorithm. Table 1 exhibits the optimal designs obtained for this problem. The optimal designs obtained using Rao algorithms are the same and are better than the other advanced optimization algorithms such as GeneAS (Genetic Adaptive Search) [25], PSO (Particle Swarm Optimization) [26], DE (Differential Evolution) [26], B&B (Branch and Bound method) [27], FA (Firefly Algorithm) [28], HSIA (Hybrid Swarm Intelligence Approach) [29], MGA (Metagenetic Algorithm) [29] and the Jaya algorithm. The Rao-2 algorithm has required less function evaluations than the other two Rao algorithms for this problem. Table 2 presents the statistical results obtained using various optimization algorithms for a helical spring problem over 30 runs. The mean best value and standard deviation of results obtained by the Rao-1 algorithm over 30 runs are better than FA and Jaya algorithm for this problem. Fig. 12 illustrates the speed of convergence of Rao algorithms to reach the optimal solution of this problem. The Rao-2 algorithm has reached first to an optimum solution of this problem as shown in Fig. 12. The comparison of results for this problem has shown the effectiveness and robustness of Rao algorithms over other considered algorithms.

In the case of a hydrostatic thrust bearing design problem, the population size and the maximum number of function evaluations are considered as 10 and 25000 respectively in each Rao algorithm. Table 3 presents the optimal designs obtained for this problem. The optimal design of this problem obtained using the Rao-2 algorithms is better than the other considered algorithms

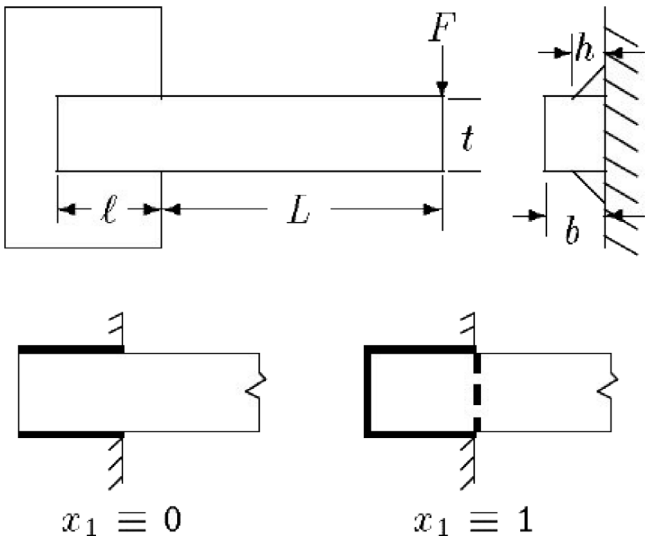

Fig. 9. Schematic diagram of a welded beam [42].

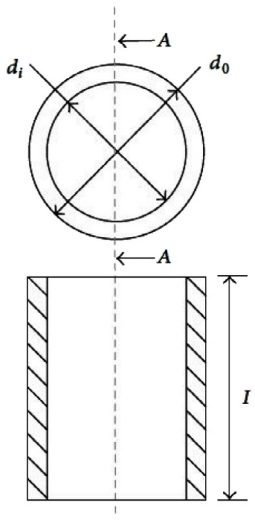

Fig. 11. Schematic diagram of a hollow shaft [45].

Table 1
Comparison of optimal designs of the helical spring obtained using Rao algorithms.

Algorithm	Volume, f_{min} (in^3)	Optimum design variables			FEs
		D (in)	d (in)	N	
GeneAS [25]	2.665	1.226	0.283	9	N.A.
PSO [26]	2.65856	1.223	0.283	9	15000
DE [26]	2.65856	1.22304	0.283	9	26000
B&B [27]	2.7995	1.1807	0.283	10	N.A.
FA [28]	2.6586	1.223049	0.283	9	50000
HSIA [29]	2.659	1.223	0.283	9	N.A.
MGA [29]	2.6681	1.2274	0.283	9	N.A.
Jaya	2.658561	1.223042	0.283	9	40580
Rao-1	**2.658559**	1.2230	0.283	9	45400
Rao-2	**2.658559**	1.2230	0.283	9	25000
Rao-3	**2.658559**	1.2230	0.283	9	52440

N.A.: Not Available.

Table 2
Comparison of statistical results of a helical spring design problem obtained over 30 runs.

Algorithm	Best f_{min} (in^3)	Mean f_{min} (in^3)	Worst f_{min} (in^3)	SD	maxFEs
FA [28]	2.658575	4.383595	7.816291	4.61E+00	75000
Jaya	2.658561	2.658698	**2.659167**	1.72E−04	75000
Rao-1	**2.658559**	**2.658675**	2.659211	**1.41E−04**	75000
Rao-2	**2.658559**	2.666750	2.699494	1.67E−02	75000
Rao-3	**2.658559**	2.665386	2.699494	1.55E−02	75000

such as PSO (Particle Swarm Optimization) [26], GASO (Genetic Algorithm aided Stochastic Optimization) [26], GeneAS (Genetic Adaptive Search) [26], BGA (Binary Genetic Algorithm) [26], ABC (Artificial Bee Colony) [21], TLBO (Teaching–Learning-Based Optimization) [21], and the Jaya algorithm [24]. Also, the Rao-2 algorithm has required less function evaluations than the other two Rao algorithms. Table 4 presents the statistical results obtained using various optimization algorithms for the hydrostatic thrust bearing problem. The mean best value and standard deviation of results obtained by the Rao-1 algorithm over 30 runs are better than ABC, TLBO, and Jaya algorithm for this problem. Fig. 13 illustrates the speed of convergence of Rao algorithms to reach the optimal solution of this problem. The Rao-2 algorithm has reached first to an optimum solution of this problem as shown in Fig. 13.

In the case of multiple disc clutch brake design problem, the population size and the maximum number of function evaluations are considered as 10 and 600 respectively in each Rao algorithm. Table 5 presents the optimal designs obtained using Rao algorithms for this problem. The optimal design of this problem obtained using each Rao algorithm is the same, but the Rao-3 algorithm has required less function evaluations than the other two Rao algorithms. Table 6 presents the statistical results obtained using various optimization algorithms for the multiple disc clutch brake problem over 30 runs. As shown in Table 6, the best design obtained using Rao algorithms is same as that given by ABC [21], TLBO [21], and Jaya algorithm [24], and better than the design obtained using the NSGA-II algorithm [30]. The

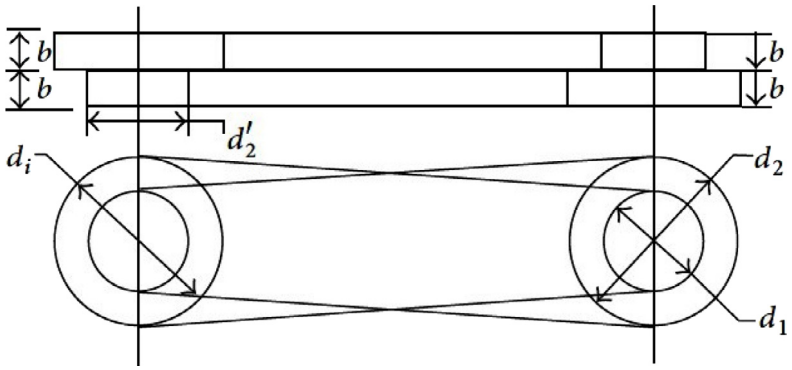

Fig. 10. Schematic diagram of a belt and pulley drive [45].

Table 3
Comparison of optimal designs of the hydrostatic thrust bearing.

Algorithm	Power loss, f_{min} (ft lb/s)	Optimum design variables				FEs
		R (in)	Ro (in)	$\mu \times 10^{-6}$ (psi s)	Q (in^3/s)	
PSO [26]	1632.2149	5.956868	5.389175	5.402133	2.301546	90000
GASO [26]	1950.286	6.271	12.901	5.605	2.938	–
GeneAS [26]	2161.4215	6.778	6.234	6.096	3.809	–
BGA [26]	2296.2119	7.7077	6.549	6.619	4.849	–
ABC [21]	1625.44276	5.95578	5.389013	5.358697	2.269655	25000
TLBO [21]	1625.443	5.95578	5.389013	5.358697	2.269655	25000
Jaya [24]	1625.44271	–	–	–	–	25000
Rao-1	1625.207058	5.955422	5.388583	5.358769	2.269461	24540
Rao-2	**1625.184754**	5.955296	5.388559	5.360411	2.270419	**24080**
Rao-3	1625.291572	5.955499	5.38871	5.359741	2.270177	24730

Table 4
Comparison of statistical results of a hydrostatic thrust bearing design problem obtained over 30 runs.

Algorithm	Best f_{min} (ft lb/s)	Mean f_{min} (ft.lb/s)	Worst f_{min} (ft lb/s)	SD	maxFEs
ABC [21]	1625.44276	1861.554	2144.836	N.A.	25000
TLBO [21]	1625.443	1797.70798	2096.80127	N.A.	25000
Jaya [24]	1625.44271	1796.89367	2104.3776	N.A.	25000
Rao-1	1625.207058	**1648.267728**	**1824.801380**	**42.530510**	25000
Rao-2	**1625.184754**	1679.441400	2209.916751	107.410308	25000
Rao-3	1625.291572	1756.501226	3403.892553	362.324314	25000

N.A.: Not Available.

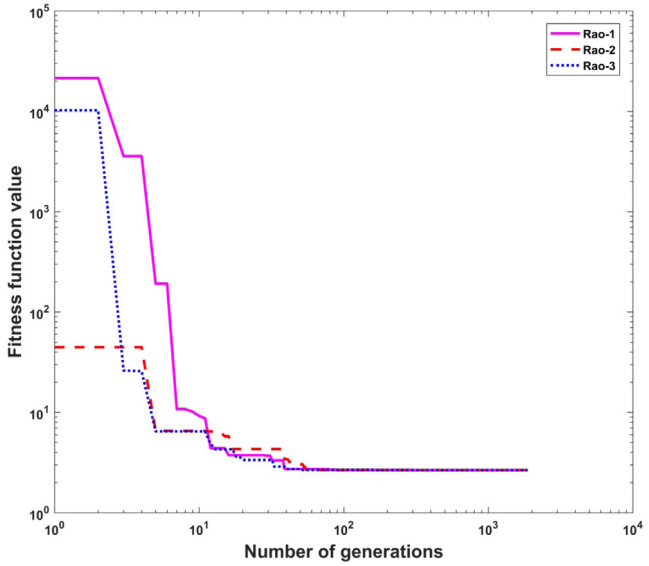

Fig. 12. A plot of convergence for the helical compression spring design problem.

mean best value and standard deviation of results obtained by the Rao-2 algorithm over 30 runs are better than ABC, TLBO, and Jaya algorithm for this problem. Fig. 14 illustrates the speed of convergence of Rao algorithms to reach the optimal solution of this problem. The Rao-3 algorithm has reached first to an optimum solution of this problem as shown in Fig. 14.

In the CRB design problem, nine different cases of CRB having different standard boundary dimensions of bearings (i.e., D, d, and B), and chamfering sizes at outer and inner raceways have been considered [31]. The results have been obtained using the Jaya algorithm also for comparison. After some trials, the population size of 10 with 5000 maximum function evaluations is considered for all nine cases of CRB. The designs obtained using Rao algorithms are compared with the design obtained using other advanced optimization algorithms such as GA [31], TLBO algorithm [32], and the Jaya algorithm. Table 7 shows the

Table 5
Optimal designs of a multiple disc clutch brake obtained using Rao algorithms.

Design variables	Algorithm		
	Rao-1	Rao-2	Rao-3
Total mass, f_{min} (kg)	**0.3136566**	**0.3136566**	**0.3136566**
r_i (mm)	70	70	70
r_o (mm)	90	90	90
t (mm)	1	1	1
F	870	870	840
Z	3	3	3
FEs	160	180	**140**
NP	10	10	10

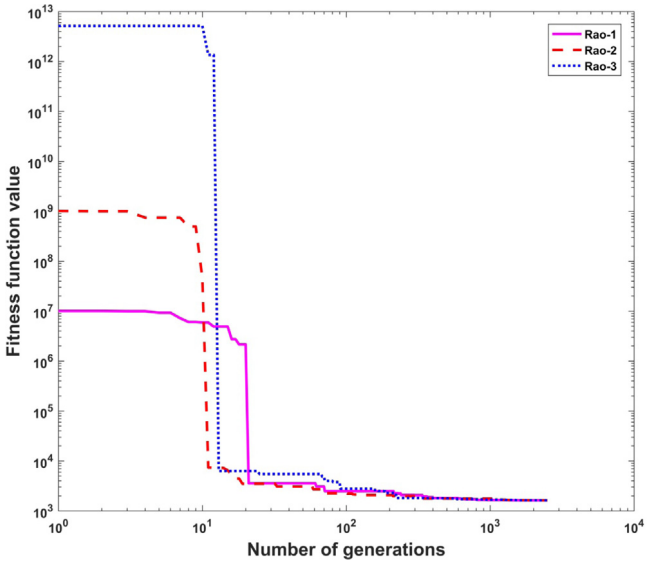

Fig. 13. A plot of convergence for the hydrostatic thrust bearing design problem.

best optimized designs of nine different types of CRB obtained using Rao algorithms and the Jaya algorithm over 30 runs. As shown in Table 7, the optimum designs obtained using considered algorithms are the same for each CRB, but the number of function

Table 6
Comparison of statistical results of a multiple disc clutch brake design problem obtained over 30 runs.

Algorithm	Best f_{min} (kg)	Mean f_{min} (kg)	Worst f_{min} (kg)	SD	maxFEs
NSGA-II [30]	0.4704	N.A.	N.A.	N.A.	N.A.
ABC [21]	0.313657	0.324751	0.352864	NA	600
TLBO [21]	0.313657	0.327166	0.392071	NA	600
Jaya [24]	**0.313657**	0.324425	0.387384	NA	600
Rao-1	**0.313657**	0.321780	0.392071	0.009985	600
Rao-2	**0.313657**	**0.315413**	**0.339999**	**0.00668**	600
Rao-3	**0.313657**	0.319783	0.392071	0.016399	600

N.A.: Not Available.

evaluations (FEs) carried out by each algorithm to reach optimum design is different. The Rao-3 algorithm required less FEs in the case of eight CRBs, whereas the Rao-2 algorithm required less FEs in the remaining one CRB.

Table 8 presents the comparison of the optimum dynamic load capacities of nine CRBs obtained using Rao algorithms and the Jaya algorithm with the results obtained by previous researchers using the GA and the TLBO algorithm. The standard values of the dynamic load capacity (C_d_std) of respective CRB [31] are also listed in Table 8 which shows that the dynamic capacities of all nine CRBs obtained using Rao algorithms are higher than those given by GA and the TLBO algorithm, and competitive with that of Jaya algorithm. A convergence plot for a second type of the CRB (i.e. NU 203) is illustrated in Fig. 15 which shows that the Rao-3 algorithm has reached first at the optimum solution of the CRB NU 203.

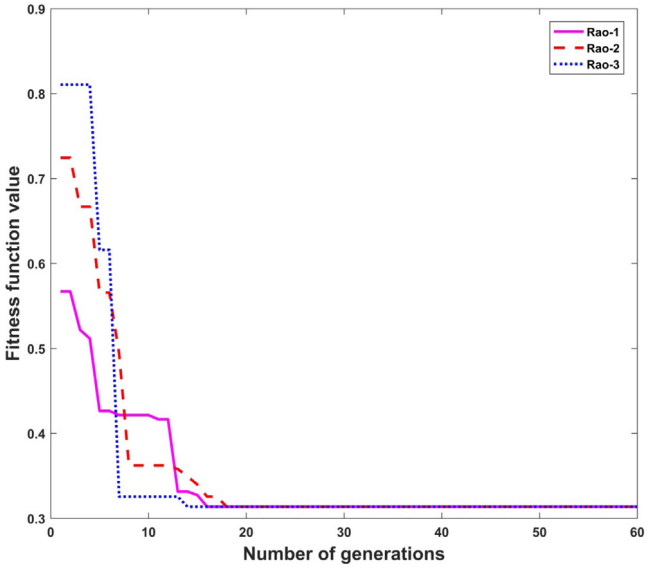

Fig. 14. A plot of convergence for the multiple disc clutch brake design problem.

In the SRB design problem, nine different cases of SRB having different standard boundary dimensions of bearings i.e., the

Table 7
Optimal designs of the cylindrical roller bearings obtained using Jaya algorithm and Rao algorithms.

Case	Bearing no.	Algorithms used	C_d (kN)	Optimized design parameters									FEs
				D_m (mm)	D_r (mm)	Z	l_e (mm)	K_{Dmin}	K_{Dmax}	e	c	β	
1	NU 202	Jaya	**23.77**	26.07	5.58	14	8.60	0.4999	0.6000	0.0300	0.3000	0.7839	4860
		Rao-1	**23.77**	26.07	5.58	14	8.60	0.4017	0.7000	0.0301	0.3000	0.8500	4030
		Rao-2	**23.77**	26.07	5.58	14	8.60	0.4656	0.6007	0.0323	0.3000	0.8500	4740
		Rao-3	**23.77**	26.07	5.58	14	8.60	0.5000	0.6213	0.0800	0.3000	0.7829	**3780**
2	NU 203	Jaya	**29.88**	29.80	6.38	14	9.60	0.4000	0.6989	0.0800	0.3000	0.8475	3940
		Rao-1	**29.88**	29.80	6.38	14	9.60	0.4000	0.6910	0.0300	0.3000	0.8500	4550
		Rao-2	**29.88**	29.80	6.38	14	9.60	0.4998	0.6036	0.0800	0.3000	0.8499	4510
		Rao-3	**29.88**	29.80	6.38	14	9.60	0.4162	0.7000	0.0300	0.3000	0.8500	**3760**
3	NU 303	Jaya	**36.68**	35.01	7.49	14	10.00	0.4621	0.6137	0.0797	0.3000	0.7381	4640
		Rao-1	**36.68**	35.01	7.49	14	10.00	0.4949	0.6000	0.0798	0.3000	0.8499	4970
		Rao-2	**36.68**	35.01	7.49	14	10.00	0.4068	0.6805	0.0500	0.3000	0.8500	4070
		Rao-3	**36.68**	35.01	7.49	14	10.00	0.4000	0.7000	0.0800	0.3000	0.8500	**3790**
4	NU 204	Jaya	**41.99**	35.01	7.49	14	11.90	0.4000	0.6000	0.0300	0.3000	0.8500	3890
		Rao-1	**41.99**	35.01	7.49	14	11.90	0.4949	0.6000	0.0800	0.3000	0.8500	3340
		Rao-2	**41.99**	35.01	7.49	14	11.90	0.4000	0.6998	0.0394	0.3000	0.8500	3130
		Rao-3	**41.99**	35.01	7.49	14	11.90	0.5000	0.7000	0.0300	0.3000	0.8500	**2610**
5	NU 304	Jaya	**49.39**	38.74	8.29	14	12.75	0.4592	0.6993	0.0418	0.3000	0.8500	4210
		Rao-1	**49.39**	38.74	8.29	14	12.75	0.4444	0.6091	0.0706	0.3000	0.8500	4180
		Rao-2	**49.39**	38.74	8.29	14	12.75	0.4658	0.7000	0.0798	0.3000	0.8500	4130
		Rao-3	**49.39**	38.74	8.29	14	12.75	0.4000	0.6185	0.0796	0.3000	0.8500	**3340**
6	NU 2205	Jaya	**53.12**	38.74	8.29	14	14.00	0.4994	0.6999	0.0300	0.3000	0.8462	4630
		Rao-1	**53.12**	38.74	8.29	14	14.00	0.4000	0.6936	0.0800	0.3000	0.8500	3930
		Rao-2	**53.12**	38.74	8.29	14	14.00	0.5000	0.7000	0.0793	0.3000	0.8336	**3620**
		Rao-3	**53.12**	38.74	8.29	14	14.00	0.4000	0.7000	0.0300	0.3000	0.8476	3640
7	NU 305	Jaya	**59.12**	46.19	9.88	14	12.60	0.4004	0.6205	0.0702	0.3000	0.7419	4910
		Rao-1	**59.12**	46.19	9.88	14	12.60	0.4000	0.6000	0.0800	0.3000	0.8500	4400
		Rao-2	**59.12**	46.19	9.88	14	12.60	0.5000	0.6000	0.0785	0.3000	0.8500	3840
		Rao-3	**59.12**	46.19	9.88	14	12.60	0.4003	0.6997	0.0800	0.3000	0.8500	**3500**
8	NU 2206	Jaya	**56.91**	46.19	9.88	14	12.00	0.5000	0.6646	0.0300	0.3000	0.7532	4410
		Rao-1	**56.91**	46.19	9.88	14	12.00	0.4853	0.6178	0.0793	0.3000	0.7693	4740
		Rao-2	**56.91**	46.19	9.88	14	12.00	0.4983	0.7000	0.0799	0.3000	0.8500	3810
		Rao-3	**56.91**	46.19	9.88	14	12.00	0.5000	0.7000	0.0445	0.3000	0.7745	**3660**
9	NU 207	Jaya	**69.42**	53.63	11.48	14	12.60	0.4025	0.6294	0.0800	0.3000	0.8500	4260
		Rao-1	**69.42**	53.63	11.48	14	12.60	0.4037	0.6997	0.0318	0.3000	0.8500	4380
		Rao-2	**69.42**	53.63	11.48	14	12.60	0.4002	0.7000	0.0800	0.3000	0.8500	4080
		Rao-3	**69.42**	53.63	11.48	14	12.60	0.4000	0.6691	0.0800	0.3000	0.8500	**3850**

Table 8
Comparison of the optimum dynamic capacities of the considered cylindrical roller bearings.

Case	Bearing no.	C_d_std [31]	Optimization algorithms					
			GA [31]	TLBO [32]	Jaya	Rao-1	Rao-2	Rao-3
1	NU 202	12.5	18.48	22.64	**23.77**	**23.77**	**23.77**	**23.77**
2	NU 203	17.2	23.58	27.16	**29.88**	**29.88**	**29.88**	**29.88**
3	NU 303	24.6	31.87	36.27	**36.68**	**36.68**	**36.68**	**36.68**
4	NU 204	25.1	32.23	39.09	**41.99**	**41.99**	**41.99**	**41.99**
5	NU 304	35.5	45.48	46.42	**49.39**	**49.39**	**49.39**	**49.39**
6	NU 2205	34.1	39.75	44.22	**53.12**	**53.12**	**53.12**	**53.12**
7	NU 305	46.5	50.39	54.44	**59.12**	**59.12**	**59.12**	**59.12**
8	NU 2206	44	51.64	52.46	**56.91**	**56.91**	**56.91**	**56.91**
9	NU 207	56	60.97	64.6	**69.42**	**69.42**	**69.42**	**69.42**

*The values of C_d are in kN.

external diameter (D), the bore diameter (d), the width (B), the corner radius of rollers (r_c) have been considered [18]. The results obtained using the Jaya algorithm are also considered for comparison. After some trials, the population size of 20 with 100 000 maximum function evaluations is considered in each SRB. The designs obtained using Rao algorithms are compared with the designs obtained using other advanced optimization algorithms such as the GA [18], hybrid ABC+GSM (Artificial Bee Colony and Grid Search Method) [46] and the Jaya algorithm. Table 9 presents the best optimized designs of nine different types of SRB obtained using Rao algorithms and the Jaya algorithm over 30 runs. As shown in Table 9, the optimum designs obtained using Rao algorithms are the same for each SRB, but FEs carried out by each algorithm to reach optimum design are different. The Rao-3 algorithm required less FEs in the case of seven CRBs, whereas the Rao-2 algorithm required less FEs in the remaining two CRBs.

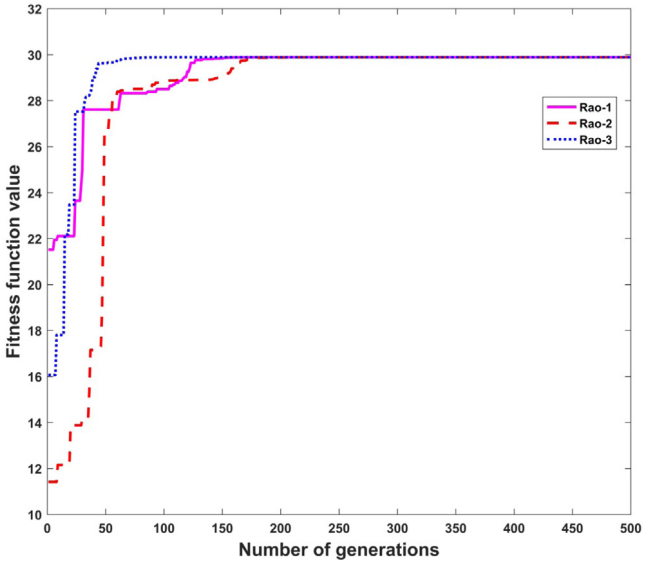

Fig. 15. A plot of convergence for the cylindrical roller bearing NU 203 design problem.

Table 9
Optimal designs of the spherical roller bearings obtained using Jaya algorithm and Rao algorithms.

Case	Bearing no.	Algorithms used	Dynamic capacity, C_d (kN)	Optimum design parameters								FEs
				D_m (mm)	D_r (mm)	Z	l_e (mm)	K_{Dmin}	K_{Dmax}	ε	α (deg.)	
1	22317	Jaya	**461.56**	162.17	15.07	31	26.08	0.2010	0.8982	0.2000	10.48	58260
		Rao-1	**461.56**	162.17	15.07	31	26.08	0.3144	0.9000	0.2000	10.48	59100
		Rao-2	**461.56**	162.17	15.07	31	26.08	0.2000	0.5042	0.2000	10.48	47980
		Rao-3	**461.56**	162.17	15.07	31	26.08	0.2009	0.8998	0.2000	10.48	**47500**
2	22310E	Jaya	**231.78**	92.89	14.54	20	16.02	0.2009	0.8065	0.2000	12.00	64480
		Rao-1	**231.78**	92.89	14.54	20	16.02	0.3981	0.8394	0.2000	12.00	62320
		Rao-2	**231.78**	92.89	14.54	20	16.02	0.3926	0.5381	0.2000	12.00	56920
		Rao-3	**231.78**	92.89	14.54	20	16.02	0.2028	0.8500	0.2000	12.00	**52840**
3	22328 CC/W33	Jaya	**1408.59**	247.84	44.24	19	36.53	0.2001	0.8991	0.2000	11.59	57180
		Rao-1	**1408.59**	247.84	44.24	19	36.53	0.4000	0.7713	0.2000	11.59	40960
		Rao-2	**1408.59**	247.84	44.24	19	36.53	0.2000	0.8695	0.2000	11.59	**51020**
		Rao-3	**1408.59**	247.84	44.24	19	36.53	0.4000	0.9000	0.2000	11.59	51600
4	22328 CC/W33400	Jaya	**2427.87**	329.74	59.54	20	46.40	0.2376	0.9000	0.2000	11.31	42920
		Rao-1	**2427.87**	329.74	59.54	20	46.40	0.4000	0.8996	0.2000	11.31	52120
		Rao-2	**2427.87**	329.74	59.54	20	46.40	0.4000	0.8999	0.2000	11.31	37020
		Rao-3	**2427.87**	329.74	59.54	20	46.40	0.2674	0.8968	0.2000	11.31	**30560**
5	24156 CC/W33	Jaya	**3357.75**	391.69	58.04	23	64.66	0.2000	0.9000	0.2000	12.00	43060
		Rao-1	**3357.75**	391.69	58.04	23	64.66	0.2000	0.9000	0.2000	12.00	41800
		Rao-2	**3357.75**	391.69	58.04	23	64.66	0.2003	0.8366	0.2000	12.00	32580
		Rao-3	**3357.75**	391.69	58.04	23	64.66	0.3852	0.9000	0.2000	12.00	**32140**
6	240/500 ECA/W33	Jaya	**6424.36**	611.64	91.51	21	85.99	0.3837	0.9000	0.2000	10.10	71920
		Rao-1	**6424.36**	611.64	91.51	21	85.99	0.3999	0.9000	0.2000	10.10	65640
		Rao-2	**6424.36**	611.64	91.51	21	85.99	0.2371	0.9000	0.2000	10.10	64780
		Rao-3	**6424.36**	611.64	91.51	21	85.99	0.2123	0.9000	0.2000	10.10	**43660**
7	240/710 ECA/W33	Jaya	**12776.84**	872.85	132.77	21	124.36	0.2000	0.9000	0.2000	10.22	51120
		Rao-1	**12776.84**	872.85	132.77	21	124.36	0.2000	0.8954	0.2000	10.22	66860
		Rao-2	**12776.84**	872.85	132.77	21	124.36	0.3998	0.8958	0.2000	10.22	48520
		Rao-3	**12776.84**	872.85	132.77	21	124.36	0.2000	0.9000	0.2000	10.22	**36060**
8	240/1060 CAF/W33	Jaya	**24573.64**	1281.33	184.48	22	175.64	0.2242	0.9000	0.2000	9.69	77420
		Rao-1	**24573.64**	1281.33	184.48	22	175.64	0.3395	0.9000	0.2000	9.69	73760
		Rao-2	**24573.64**	1281.33	184.48	22	175.64	0.2000	0.9000	0.2000	9.69	68140
		Rao-3	**24573.64**	1281.33	184.48	22	175.64	0.3971	0.9000	0.2000	9.69	**48580**
9	241/1000 ECAF/W33	Jaya	**33081.77**	1338.87	204.84	21	233.61	0.2000	0.8475	0.2000	12.00	74400
		Rao-1	**33081.77**	1338.87	204.84	21	233.61	0.2221	0.9000	0.2000	12.00	49200
		Rao-2	**33081.77**	1338.87	204.84	21	233.61	0.3873	0.9000	0.2000	12.00	**24800**
		Rao-3	**33081.77**	1338.87	204.84	21	233.61	0.2032	0.8941	0.2000	12.00	38880

Table 10
Comparison of the optimum dynamic capacities of the considered spherical roller bearings.

Bearing no.	C_d_std [18]	Optimization algorithms					
		Hybrid ABCA + GSM [46]	GA [18]	Jaya	Rao-1	Rao-2	Rao-3
22317	399.3	435.98	439.1	**461.56**	**461.56**	**461.56**	**461.56**
22310E	220	227.55	231	**231.78**	**231.78**	**231.78**	**231.78**
22328 CC/W33	1290	1369.1	1400.2	**1408.59**	**1408.59**	**1408.59**	**1408.59**
22328 CC/W33400	2120	2264.6	2345.2	**2427.87**	**2427.87**	**2427.87**	**2427.87**
24156 CC/W33	3100	3119	3350.6	**3357.75**	**3357.75**	**3357.75**	**3357.75**
240/500 ECA/W33	4770	6313	6387.4	**6424.36**	**6424.36**	**6424.36**	**6424.36**
240/710 ECA/W33	9370	12349	12642.7	**12776.84**	**12776.84**	**12776.84**	**12776.84**
240/1060 CAF/W33	17300	22010	24235.6	**24573.64**	**24573.64**	**24573.64**	**24573.64**
241/1000 ECAF/W33	26700	31304	33065.3	**33081.77**	**33081.77**	**33081.77**	**33081.77**

*The values of C_d are in kN.

Table 11
Comparison of the optimum designs of the plate fin heat exchanger.

Design parameters	Original design [33]	Optimization algorithms							
		GA [34]	BA [35]	ICA [34]	FOA [36]	Jaya	Rao-1	Rao-2	Rao-3
f_{min} (N_s)	0.1576	0.1416	0.1341	0.1374	0.1333	0.116665	0.116597	**0.116546**	0.116547
L_h (m)	0.3	0.95	0.997	1	0.9	1	1	1	1
L_c (m)	0.3	0.44	0.94	0.88	1	0.64	0.68	0.65	0.66
H (mm)	2.49	7.2	8.33	5	8.6	9.82	9.82	9.82	9.82
n (fins/m)	782	417	257.02	240	265.2	551.52	548.02	544.54	541.69
t (mm)	0.1	0.1	0.166	0.19	0.1	0.11	0.12	0.12	0.12
l (mm)	3.18	7.2	9.51	9.6	7.2	9.55	10.00	10.00	10.00
N_h	167	57	56	77	53	48	48	48	48
ΔP_h (kPa)	9.34	4.2	0.741	1.23	0.656	3.11	3.02	2.95	2.90
ΔP_c (kPa)	6.9	0.52	0.46	0.67	0.589	0.80	0.80	0.80	0.80
L_{noflow}	1	0.87	0.997	0.87	0.976	1.000	1.000	1.000	1.000
ε	–	0.821	0.826	0.821	0.827	0.874	0.874	0.874	0.874
FEs	–	NA	NA	NA	NA	13870	13720	**13000**	13780

Table 12
Statistical results of a plate fin heat exchanger design problem obtained using Jaya algorithm and Rao algorithms over 30 runs.

Algorithm	Best f_{min}	Mean f_{min}	Worst f_{min}	SD
Jaya	0.116665	0.117064	**0.120385**	9.19E−04
Rao-1	0.116597	**0.116922**	**0.120385**	**6.75E−04**
Rao-2	**0.116546**	0.226149	2.484056	4.43E−01
Rao-3	0.116547	0.137704	0.425428	7.82E−02

Table 10 presents the comparison of the optimum dynamic load capacities of nine SRBs obtained using Rao algorithms and the Jaya algorithm with the results obtained by previous researchers using GA and hybrid ABCA–GSM algorithm. The values of the standard dynamic load capacity (C_d_std) of respective SRB [18] are also listed in Table 9 which shows that the dynamic capacities of all nine SRBs obtained using Rao algorithms are superior to those given by GA and hybrid ABC–GSM algorithm, and competitive with that of Jaya algorithm. A convergence plot of C_d for a second type of the SRB (i.e. 22310E) is illustrated in Fig. 16 which shows that the Rao-3 algorithm has reached first at optimum C_d of the second SRB (22310E).

In the case of a plate fin heat exchanger design problem, the population size and the maximum number of function evaluations are considered as 10 and 14 000 respectively in each Rao algorithm. Table 11 exhibits the optimal designs obtained for this problem. The optimal design obtained using the Rao-2 algorithm is superior to the designs obtained by other advanced optimization algorithms such as GA (Genetic Algorithm) [34], BA (Bees Algorithm) [35], ICA (Imperialist Competitive Algorithm) [34], FOA (Falcon Optimization Algorithm) [36], and the Jaya algorithm. The Rao-2 algorithm has required less function evaluations than the other two Rao algorithms for this problem. Table 12 presents the statistical results obtained using Rao algorithms and the Jaya algorithm for this problem over 30 runs. The mean best value and standard deviation of results obtained by the Rao-1 algorithm

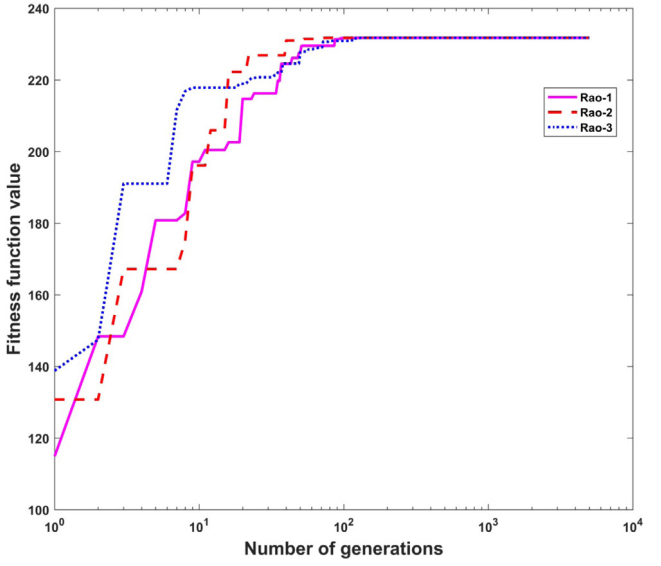

Fig. 16. A plot of convergence for the spherical roller bearing 22310E design problem.

over 30 runs are found the better than other two Rao algorithms and the Jaya algorithm for this problem. Fig. 17 illustrates the speed of convergence of Rao algorithms to reach the optimal solution of this problem. The Rao-2 algorithm has reached first to an optimum solution of this problem as shown in Fig. 17. The comparison of results for this problem has shown the effectiveness of Rao algorithms over the other algorithms presented by the previous researchers.

In the case of a shell-and-tube heat exchanger design problem, the population size and the maximum number of function evaluations are considered as 10 and 6000 respectively in each

Table 13
Comparison of the optimum designs of the shell-and-tube heat exchanger.

Design parameters	Original design [37]	Algorithms								
		GA [38]	ABC [39]	PSO [40]	BBO [41]	FOA [36]	Jaya	Rao-1	Rao-2	Rao-3
f_{min} **(Ctot), €**	43989	20834	19478	20310	19310	18560.3	**18335.99**	**18335.99**	**18335.99**	**18335.99**
C_i (€)	16549	19163	17893	18614	18059	16723	16070.67	16070.69	16070.68	16070.69
Cod (€)	27440	1671	1584.2	1696	1251.5	1837.3	2265.32	2265.29	2265.31	2265.30
d_o (m)	0.013	0.016	0.0103	0.0145	0.01	0.012	0.012	0.012	0.012	0.012
D_s (m)	0.387	0.62	1.0024	0.59	0.55798	0.52	0.4637	0.4637	0.4637	0.4637
B (m)	0.305	0.44	0.354	0.423	0.5	0.5	0.5	0.5	0.5	0.5
L (m)	4.88	1.548	2.4	1.45	1.133	1.2316	1.3912	1.3912	1.3912	1.3912
N_t	160	803	704	894	1565	1017	870	870	870	870
v_t (m/s)	1.76	0.68	0.36	0.74	0.898	0.958	1.2261	1.2261	1.2261	1.2261
Re_t	36400	9487	–	9424	7804	10000	12205.2	12205.2	12205.2	12205.2
Pr_t	6.2	6.2	–	6.2	6.2	6.2	6.2026	6.2026	6.2026	6.2026
h_t (W/m^2 K)	6558	6043	4438	5618	9180	9317.3	6687	6687	6687	6687
ΔP_t (Pa)	62812	3673	2046	4474	4176	4591	5412	5412	5412	5412
De (m)	0.013	0.011	–	0.0103	0.0071	0.0086	0.01	0.01	0.01	0.01
v_s (m/s)	0.94	0.41	0.12	0.375	0.398	0.4265	0.4783	0.4783	0.4783	0.4783
Re_s	16200	8039	–	4814	3515	4568	4904	4904	4904	4904
Pr_s	67684	5.4	–	5.4	5.4	5.4	5.4	5.3935	5.3935	5.3935
h_s (W/m^2 K)	5735	3476	5608	4088.3	4911	4682.6	5613	5613	5613	5613
ΔP_s (Pa)	67684	4365	2716	4721	5917	5523	7171	7171	7171	7171
U (W/m^2 K)	1471	1121	1187	1177	1384	1369.5	1591	1591	1591	1591
A (m^2)	46.6	62.5		59.15	55.73	47.65	44	44	44	44
FEs		NA	NA	NA	NA	NA	5270	4660	5060	**3160**

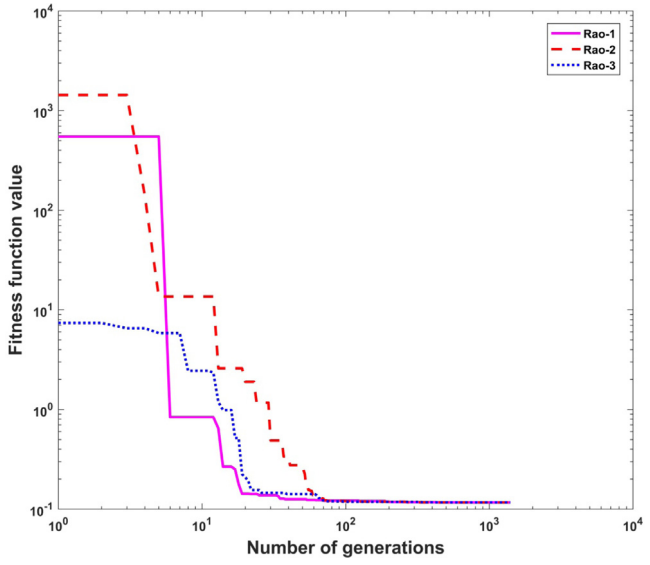

Fig. 17. A plot of convergence for the plate fin heat exchanger design problem.

Rao algorithm. Table 13 shows the optimal designs obtained for this problem. The optimal designs obtained using Rao algorithms and the Jaya algorithm are nearly the same and superior to other advanced optimization algorithms such as GA (Genetic Algorithm) [38], ABC (Artificial Bee Colony) [39], PSO (Particle Swarm Optimization) [40], BBO (Biogeography-based Optimization) [41], and FOA (Falcon Optimization Algorithm) [36]. The Rao-3 algorithm has required less function evaluations than the other two Rao algorithms for this problem. Table 14 presents the statistical results obtained using Rao algorithms and the Jaya algorithm for this problem over 30 runs. The mean best value and standard deviation of results obtained by the Rao-1 algorithm over 30 runs are better than the other two Rao algorithms and the Jaya algorithm for this problem. Fig. 18 illustrates the speed of convergence of Rao algorithms to reach the optimal solution of this problem. The Rao-3 algorithm has reached first to an optimum solution of this problem as shown in Fig. 18.

In a welded beam problem, the population size and the maximum number of function evaluations are considered as 10 and

Table 14
Statistical results of a shell-and-tube heat exchanger design problem obtained using Jaya algorithm and Rao algorithms over 30 runs.

Algorithm	Best Ctot (€)	Mean Ctot (€)	Worst Ctot (€)	SD
Jaya	18335.99	18336.08	18336.45	8.45E−02
Rao-1	**18335.99**	**18336.06**	**18336.29**	**5.77E−02**
Rao-2	18335.99	18342.70	18435.56	2.52E+01
Rao-3	18335.99	18342.69	18435.56	2.52E+01

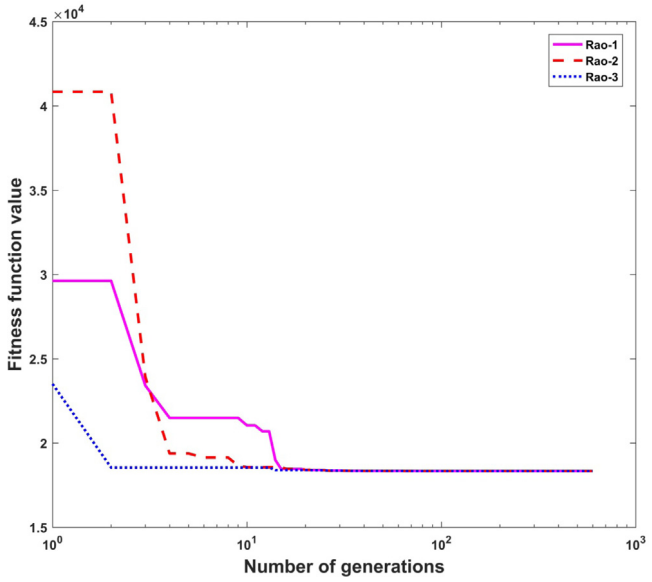

Fig. 18. A plot of convergence for the shell-and-tube heat exchanger design problem.

5000 respectively in each Rao algorithm. Table 15 presents the optimal designs obtained for this problem. The optimal designs obtained using Rao algorithms and the Jaya algorithm are the same and superior to the other considered optimization algorithms such as, GeneAS and PSO. The Rao-3 algorithm has required less function evaluations than the other two Rao algorithms for this problem. Table 16 presents the statistical results obtained using Rao algorithms and the Jaya algorithm for this

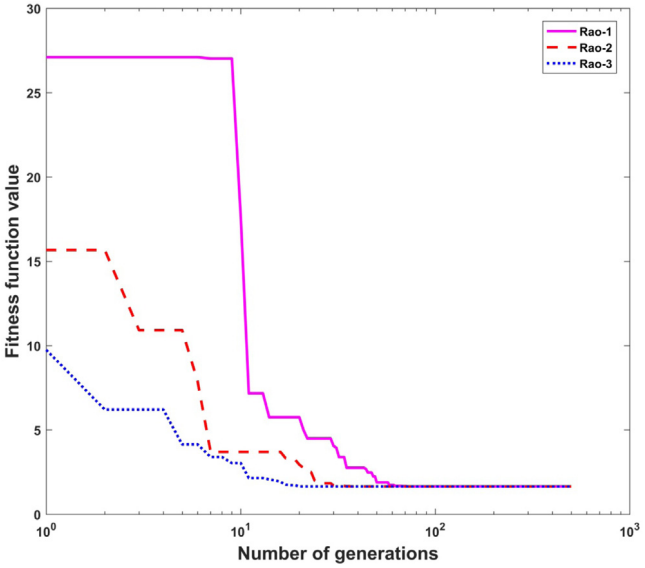

Fig. 19. A plot of convergence for the welded beam design problem.

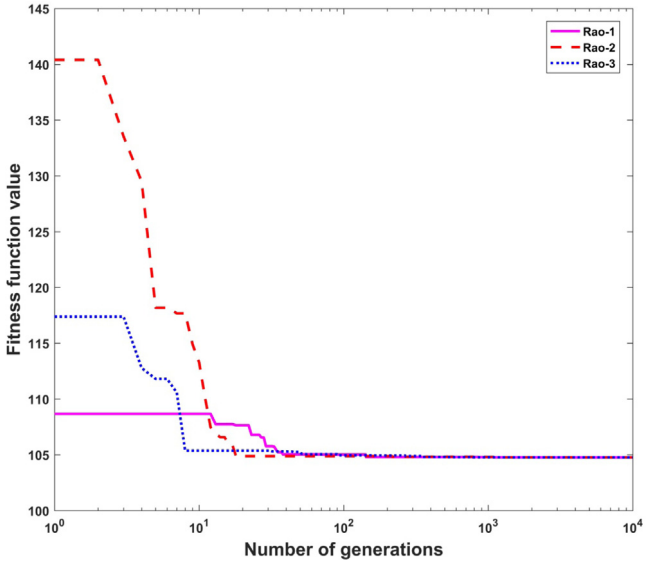

Fig. 20. A plot of convergence for the belt–pulley drive design problem.

Table 15
Comparison of optimal designs of the welded beam obtained using Rao algorithms.

Algorithm	Cost, f_{min}	Optimum design variables						FEs
		x_1	x_2	h (in)	t (in)	b (in)	l (in)	
GeneAS [42]	1.9422	1	1	0.1875	8.25	0.25	1.6849	NA
PSO [43]	2.025363	1	1	0.125	8.3125	0.25	4.115994	NA
PSO [44]	1.955301	1	1	0.1875	8.25	0.25	1.782103	NA
Jaya	**1.647757**	1	1	0.125	8.25	0.25	1	1580
Rao-1	**1.647757**	1	1	0.125	8.25	0.25	1	730
Rao-2	**1.647757**	1	1	0.125	8.25	0.25	1	370
Rao-3	**1.647757**	1	1	0.125	8.25	0.25	1	**300**

Table 16
Statistical results of a welded beam design problem obtained using Jaya algorithm and Rao algorithms over 30 runs.

Algorithm	Best cost	Mean cost	Worst cost	SD	maxFEs
Jaya	**1.647757**	1.895313	2.827328	0.380463	5000
Rao-1	**1.647757**	1.857358	2.821862	0.377552	5000
Rao-2	**1.647757**	**1.832341**	2.296429	**0.183766**	5000
Rao-3	**1.647757**	1.853049	**2.220598**	0.212436	5000

problem over 30 runs. The mean best value and the standard deviation of results obtained by the Rao-2 algorithm over 30 runs are better than other two Rao algorithms and the Jaya algorithm for this problem. Fig. 19 illustrates the speed of convergence of Rao algorithms to reach the optimal solution of this problem. The Rao-3 algorithm has reached first to an optimum solution of this problem as shown in Fig. 19.

Table 18
Statistical results of a belt–pulley drive design problem obtained using Jaya algorithm and Rao algorithms over 30 runs.

Algorithm	Best f_{min} (kg)	Mean f_{min} (kg)	Worst f_{min} (kg)	SD	maxFEs
Jaya	104.761253	104.764564	104.770193	2.32E−03	100 000
Rao-1	**104.761153**	**104.764493**	**104.770168**	**2.18E−03**	100 000
Rao-2	104.761290	104.798754	105.000837	8.08E−02	100 000
Rao-3	104.761518	104.872199	106.096094	3.38E−01	100 000

In the belt–pulley drive design problem, the population size and the maximum number of function evaluations are considered as 10 and 100 000 respectively in each Rao algorithm. Table 17 presents the optimal designs obtained for this problem. The optimal design obtained using the Rao-1 algorithm is better than the other optimization algorithms such as GA and the Jaya algorithm. Table 18 presents the statistical results obtained using Rao algorithms and the Jaya algorithm for this problem over 30 runs. The mean best value and standard deviation of results obtained by the Rao-1 algorithm over 30 runs are found better than the other two Rao algorithms and the Jaya algorithm for this problem. Fig. 20 illustrates the speed of convergence of Rao algorithms to reach the optimal solution of this problem. The Rao-1 algorithm has reached first to an optimum solution of this problem as shown in Fig. 20.

In the hollow shaft design problem, the population size and the maximum number of function evaluations are considered as 10 and 5000 respectively in each Rao algorithm. Table 19 presents the optimal designs obtained for this problem. The optimal designs obtained using Rao algorithms and the Jaya algorithm

Table 17
Comparison of optimal designs of the belt–pulley drive obtained using Rao algorithms.

Design parameters	Conventional design [45]	Algorithm				
		GA [45]	Jaya	Rao-1	Rao-2	Rao-3
f_{min} (W, kg)	105.12	104.533508 (104.762898[a])	104.761253	**104.761153**	104.761290	104.761518
d_1 (cm)	21.12	20.957056	21.006918	20.998852	21.009089	20.970888
d_2 (cm)	73.25	72.906562	72.732264	72.760100	72.724478	72.857216
b (cm)	5.21	5.239177	5.251730	5.249720	5.252303	5.242720
d'_1 (cm)	42.25	42.370429	42.013835	41.997704	42.018177	41.941777
d'_2 (cm)	36.60	36.453281	36.366132	36.380050	36.362239	36.428608
FEs	–	300000	86110	51300	35280	88460

[a]Actual value of f_{min} for the design variables presented by [45].

Table 19
Comparison of optimal designs of the hollow shaft obtained using Rao algorithms.

Design parameters	Conventional design [45]	Algorithm				
		GA [45]	Jaya	Rao-1	Rao-2	Rao-3
f_{min} (W, kg)	2.4017	2.370429	**2.370398**	**2.370398**	**2.370398**	**2.370398**
d_o (cm)	10.9	11.092836	11.092972	11.092972	11.092972	11.092972
k	0.9685	0.9699	0.97	0.97	0.97	0.97
FEs	–	300000	1360	1520	1000	**960**

Table 20
Statistical results of a hollow shaft obtained using Jaya algorithm and Rao algorithms over 30 runs.

Algorithm	Best f_{min} (kg)	Mean f_{min} (kg)	Worst f_{min} (kg)	SD	maxFEs
Jaya	**2.370398**	**2.370398**	**2.370398**	**0**	5000
Rao-1	**2.370398**	**2.370398**	**2.370398**	**0**	5000
Rao-2	**2.370398**	**2.370398**	**2.370398**	**0**	5000
Rao-3	**2.370398**	**2.370398**	**2.370398**	**0**	5000

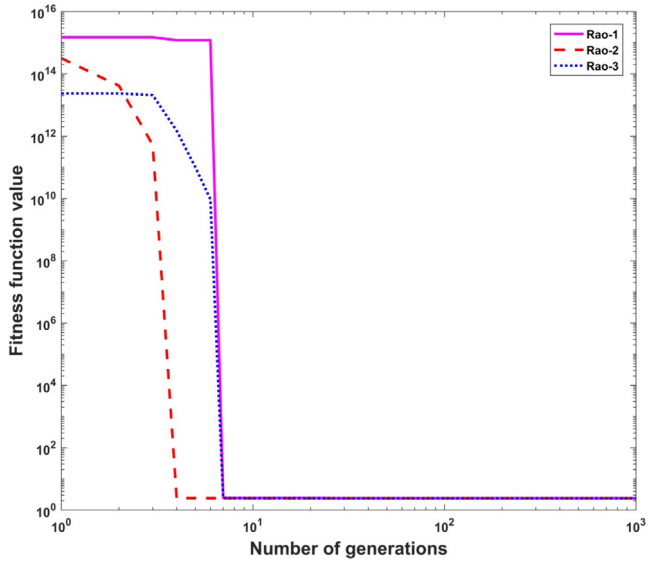

Fig. 21. A plot of convergence for the hollow shaft design problem.

are the same and better than the GA. The Rao-3 algorithm has required less function evaluations than the other two Rao algorithms for this problem. Table 20 shows that the statistical results obtained using Rao algorithms and the Jaya algorithm for this problem over 30 runs are the same. As the standard deviation of results obtained by Rao algorithms over 30 runs is exactly zero, it can be said that the Rao algorithms have reached the best optimum solution in each run. Fig. 21 illustrates the speed of convergence of Rao algorithms to reach the optimal solution of this problem. The Rao-3 algorithm has reached first to optimum solution of this problem as shown in Fig. 21.

The comparison of results shows the ability and effectiveness of Rao algorithms to solve constrained design optimization problems. The next section presents the conclusions of this work.

5. Conclusions

In this work, the performance of the proposed Rao algorithms is explored over ten complex design optimization problems of different mechanical system components. From the comparison of results, it can be concluded that Rao algorithms are effective and robust than the other optimization algorithms considered by the previous researchers for solving the complex constrained design problems of mechanical system components considered. Rao algorithms are very simple and independent of any metaphors and algorithm-specific control parameters. The computational efforts are decreased with the help of Rao algorithms to solve complex design optimization problems. In addition, Rao algorithms are found computationally inexpensive because of less time taken by the Rao algorithms to execute. Also, the Rao algorithms have the potential to handle mixed-type design variables simultaneously while satisfying several complex design constraints. In future studies, these Rao algorithms can be used to solve other design optimization problems of mechanical components. Also, the multi-objective design optimization problems of mechanical components can be solved using the proposed Rao algorithms.

Declaration of competing interest

No author associated with this paper has disclosed any potential or pertinent conflicts which may be perceived to have impending conflict with this work. For full disclosure statements refer to https://doi.org/10.1016/j.asoc.2020.106141.

CRediT authorship contribution statement

R.V. Rao: Methodology. **R.B. Pawar:** Validation.

Appendix

Formulations of the considered design optimization problems of mechanical system components

1. Helical compression spring

$$\text{Design variables, } \{x\} = [D, d, n] \tag{A.1}$$

$$\text{Objective function: } f(x) = \frac{\pi^2 D d^2 (n+2)}{4} \tag{A.2}$$

Design constraints:

$$C_1(x) = S - \frac{8KP_{max}D}{\pi d^3} \geq 0 \tag{A.3}$$

$$C_2(x) = l_{free} - [\delta + 1.05(n+2)d] \geq 0 \tag{A.4}$$

$$C_3(x) = d - d_{min} \geq 0 \tag{A.5}$$

$$C_4(x) = D_{max} - D - d \geq 0 \tag{A.6}$$

$$C_5(x) = \frac{(D-d)}{d} - 3 \geq 0 \tag{A.7}$$

$$C_6(x) = \delta_{pm} - \delta_p \geq 0 \tag{A.8}$$

$$C_7(x) = l_{free} - \delta - \left(\frac{P_{max} - P_{load}}{k}\right) - 1.05(N+2)d \geq 0 \tag{A.9}$$

$$C_8(x) = \left(\frac{P_{max} - P_{load}}{k}\right) - \delta_w \geq 0 \tag{A.10}$$

$$K = \frac{4C-1}{4C-4} + \frac{0.615}{C}; \quad C = \frac{D}{d}; \quad \delta = \frac{8P_{max}D^3N}{GD^4}; \tag{A.11}$$

$$k = \frac{Gd^4}{8ND^3}; \quad \delta_p = \frac{F_p}{k} \tag{A.12}$$

$$P_{max} = 1000\,\text{lb}, P_{load} = 300\,\text{lb}, S = 189\,\text{KPsi}, E = 30\,\text{MPsi}, \tag{A.13}$$

$$G = 11.5\,\text{MPsi}, L_{free} = 14\,\text{in}, d_{min} = 0.2\,\text{in}, D_{max} = 3\,\text{in}, \tag{A.14}$$

$$\delta_{pm} = 6\,in, \delta_w = 1.25\,in. \tag{A.15}$$

2. Hydrostatic thrust bearing

Design variables, $\{x\} = [R, R_o, Q, \mu]$ (A.16)

Objective function: $f(x) = \frac{QP_o}{0.7} + E_f$ (A.17)

Design constraints:

$$C_1(x) = W - W_s \geq 0 \tag{A.18}$$

$$C_2(x) = p_{max} - p_o \geq 0 \tag{A.19}$$

$$C_3(x) = \Delta T_{max} - \Delta T \geq 0 \tag{A.20}$$

$$C_4(x) = h - h_{min} \geq 0 \tag{A.21}$$

$$C_5(x) = R - R_o \geq 0 \tag{A.22}$$

$$C_6(x) = 0.001 - \frac{\gamma}{gP_o}\left(\frac{Q}{2\pi Rh}\right) \geq 0 \tag{A.23}$$

$$C_7(x) = 5000 - \frac{W}{\pi(R^2 - R_o^2)} \geq 0 \tag{A.24}$$

$$W = \frac{P_o\pi}{2}\frac{(R^2 - R_o^2)}{\ln\frac{R}{R_o}}; P_o = \frac{6\mu Q}{\pi h^3}\ln\frac{R}{R_o}; \tag{A.25}$$

$$E_f = 9336Q\gamma c\Delta T; \Delta T = 2(10^p - 560) \tag{A.26}$$

$$P = \log_{10}\log_{10}(8.112e6\mu + 0.8) - C_1 \tag{A.27}$$

$$h = \left(\frac{2\pi N}{60}\right)^2 \frac{2\pi\mu}{E_f}\left(\frac{R^4}{4} - \frac{R_o^4}{4}\right) \tag{A.28}$$

$$\gamma = 0.0307, C = 0.5, n = -3.55, C_1 = 10.04, W_s = 101{,}000 \tag{A.29}$$

$$P_{max} = 1000, \Delta T_{max} = 50, h_{min} = 0.001, g = 386.4, N = 750 \tag{A.30}$$

$$1 \leq R, R_o, Q \leq 16, 1e^{-1} \leq \mu \leq 16e^{-6} \tag{A.31}$$

3. Multiple disc clutch brake

Design variables, $\{x\} = [r_o, r_i, t, F, Z]$ (A.32)

Objective function: $f(x) = \pi\left(r_o^2 - r_i^2\right)t(z+1)\rho$ (A.33)

Design constraints:

$$C_1(x) = r_o - r_i - \Delta r \geq 0 \tag{A.34}$$

$$C_2(x) = l_{max} - (z+1)(t+\delta) \geq 0 \tag{A.35}$$

$$C_4(x) = p_{max} - p_{rz} \geq 0 \tag{A.36}$$

$$C_5(x) = p_{max}v_{srmax} - p_{rz}v_{sr} \geq 0 \tag{A.37}$$

$$C_6(x) = v_{srmax} - v_{sr} \geq 0 \tag{A.38}$$

$$C_7(x) = T_{max} - T \geq 0 \tag{A.39}$$

$$C_8(x) = M_h - sM_s \geq 0 \tag{A.40}$$

$$C_9(x) = T \geq 0 \tag{A.41}$$

$$M_h = \frac{2}{3}\mu FZ\frac{r_o^3 - r_i^3}{r_o^2 - r_i^2}; p_{rz} = \frac{F}{\pi\left(r_o^2 - r_i^2\right)}; \tag{A.42}$$

$$v_{sr} = \frac{2\pi n(r_o^3 - r_i^3)}{90(r_o^2 - r_i^2)}; T = \frac{l_z\pi n}{30(M_h + M_f)}; \tag{A.43}$$

$$r_i \in (60, 61, 62, \ldots\ldots\ldots\ldots\ldots, 80) \tag{A.44}$$

$$r_i \in (90, 91, 92, \ldots\ldots\ldots\ldots\ldots, 110) \tag{A.45}$$

$$t \in (1, 1.5, 2, 2.5, 3) \tag{A.46}$$

$$F_1 \in (600, 610, 620, \ldots\ldots\ldots\ldots, 1000) \tag{A.47}$$

$$z \in (2, 3, 4, 5, \ldots\ldots\ldots\ldots, 9) \tag{A.48}$$

$$\Delta r = 20\text{ mm}, t_{max} = 3\text{ mm}, t_{min} = 1\text{ mm}, \mu = 0.5, s = 0.5 \tag{A.49}$$

$$M_s = 40\text{ N m}, M_f = 3\text{ N m}, n = 250\text{ rpm}, \quad p_{max} = 1\text{ MPa}, l_z = 55\text{ kg m}^2 \tag{A.50}$$

$$T_{max} = 15\text{ s}, F_{max} = 1000\text{ N}, r_{imin} = 60\text{ mm}, r_{omax} = 110\text{ mm} \tag{A.51}$$

$l_{max} = 30$ mm, $Z_{max} = 10$, $v_{srmax} = 10$ m/s (A.52)

4. Cylindrical roller bearing

Design variables,

$$\{X\} = [D_r, D_m, l_e, Z, K_{Dmin}, K_{Dmax}, e, \varepsilon, \beta] \quad \text{(A.53)}$$

Objective function:

$$C_d = 207.9 b_m \lambda v \left[1 + \left\{1.04\left(\frac{1-\gamma}{1+\gamma}\right)^{143/108}\right\}^{9/2}\right]^{-2/9} \times \frac{\gamma^{2/9}(1-\gamma)^{29/27}}{(1+\gamma)^{1/4}} (i l_e)^{7/9} D_r^{29/27} Z^{3/4} \quad \text{(A.54)}$$

where,

$$\gamma = \frac{D_r}{D_m} \quad \text{(A.55)}$$

$$f(X) = \max(C_d) \quad \text{(A.56)}$$

Design constraints:

$$g_1(X) = D_m \geq (2r_{3\min} + d) \quad \text{(A.57)}$$

$$g_2(X) = (D - 2r_{1\min}) \geq D_m(24) \quad \text{(A.58)}$$

$$g_3(X) = D_r - D_{r_{LL}} \geq 0 \quad \text{(A.59)}$$

$$g_4(X) = D_{r_{UL}} - D_r \geq 0 \quad \text{(A.60)}$$

where

$$D_{r_{LL}} - \frac{268.71\sqrt{Q_{\max}\chi}}{\sigma_{safe}} \text{ and } D_{r_{UL}} = 0.5[(D - 2r_{1\min}) - (d + 2r_{3\min})] \quad \text{(A.61)}$$

$$g_5(X) = Z \geq \frac{\pi(d + 2r_{3\min})}{D_{r_{UL}}} \quad \text{(A.62)}$$

$$g_6(X) = \frac{\pi(D - 2r_{1\min})}{D_{r_{LL}}} \geq Z \quad \text{(A.63)}$$

$$g_7(X) = 2D_r - K_{D\min}(D - d) \geq 0 \quad \text{Here,} \quad 0.4 \leq K_{D\min} \leq 0.5 \quad \text{(A.64)}$$

$$g_8(X) = K_{D\max}(D - d) - 2D_r \geq 0 \quad \text{Here,} \quad 0.6 \leq K_{D\max} \leq 0.7 \quad \text{(A.65)}$$

$$g_9(X) = D_m - (D + d)(0.5 - e) \geq 0 \quad \text{Here,} \quad 0.03 \leq e \leq 0.08 \quad \text{(A.66)}$$

$$g_{10}(X) = (D + d)(0.5 + e) - D_m \geq 0 \quad \text{(A.67)}$$

$$g_{11}(X) = 0.5(D - D_m - D_r) - \varepsilon D_r \geq 0 \quad \text{Here,} \quad 0.3 \leq \varepsilon \leq 0.4 \quad \text{(A.68)}$$

$$g_{12}(X) = 0.5(D - D_o) - 2r_{1\min} \geq 0 \quad \text{Here,} \quad D_o = D_m + D_r \quad \text{(A.69)}$$

$$g_{13}(X) = 0.5(D_i - d) - 0.5(D - D_o) \geq 0 \quad \text{Here,} \quad D_i = D_m - D_r \quad \text{(A.70)}$$

$$g_{14}(X) = \sigma_{c_{safe}} - \sigma_{c_{\max}}^{li} \geq 0 \quad \text{(A.71)}$$

where,

$$\sigma_{c_{safe}} = 4000 \text{ MPa}; \quad \sigma_{c_{\max}}^{li} = \frac{2Q_{\max_i}}{\pi l_e b_i} \quad \text{(A.72)}$$

$$b_i = 3.35 \times 10^{-3}\left(\frac{Q_{\max_i}}{l_e \sum \rho_i}\right)^{1/2}; \quad \sum \rho_i = \frac{2}{D_r} + \frac{2}{D_i} \quad \text{(A.73)}$$

$$g_{15}(X) = \sigma_{c_{safe}} - \sigma_{c_{\max}}^{lo} \geq 0 \quad \text{(A.74)}$$

where,

$$\sigma_{c_{safe}} = 4000 \text{ MPa}; \quad \sigma_{c_{\max}}^{lo} = \frac{2Q_{\max_o}}{\pi l_e b_o} \quad \text{(A.75)}$$

$$b_o = 3.35 \times 10^{-3}\left(\frac{Q_{\max_o}}{l_e \sum \rho_o}\right)^{1/2}; \sum \rho_o = \frac{2}{D_r} - \frac{2}{D_o} \quad \text{(A.76)}$$

$$g_{16}(X) = 2\pi - 2Z\sin^{-1}\left(D_r \Big/ D_m\right) \geq Z\left(\pi \Big/ 180\right) \quad \text{(A.77)}$$

$$g_{17}(X) = \beta B \geq l_e \quad \text{Here, } 0.7 \leq \beta \leq 0.85 \quad \text{(A.78)}$$

$$g_{18}(X) = B - l_e - 2r \geq 2r_1 \quad \text{(A.79)}$$

$$g_{19}(X) = 0.5(D - D_o) \geq 3Z_{static} \quad \text{Here,} \quad Z_{static} = 0.626 b_o \quad \text{(A.80)}$$

5. Spherical roller bearing

Design variables,

$$\{X\} = [D_r, D_m, l_e, Z, \alpha, K_{Dmin}, K_{Dmax}, \varepsilon] \quad \text{(A.81)}$$

Objective function:

$$C_d = 207.9 b_m \lambda v \left[1 + \left\{1.04\left(\frac{1-\gamma}{1+\gamma}\right)^{143/108}\right\}^{9/2}\right]^{-2/9} \times \frac{\gamma^{2/9}(1-\gamma)^{29/27}}{(1+\gamma)^{1/4}} (i l_e \cos\alpha)^{7/9} Z^{3/4} D_r^{29/27} \quad \text{(A.82)}$$

where

$$\gamma = \frac{D_r \cos\alpha}{D_m} \quad \text{(A.83)}$$

$$f_1(X) = \max(C_d) \quad \text{(A.84)}$$

Design constraints:

$$g_1(X) = D_m \geq (D_r \cos\alpha + d + 2r_c) \quad \text{(A.85)}$$

$$g_2(X) = (D - D_r \cos\alpha - 2r_c) \geq D_m \quad \text{(A.86)}$$

$$g_3(X) = D_r - D_{r_{LL}} \geq 0 \tag{A.87}$$

$$D_{r_{LL}} = \frac{268.71\sqrt{Q_{\max}\chi}}{\sigma_{safe}}; \quad \chi = \frac{D_r}{l_e}; \tag{A.88}$$

$$D_{r_{UL}} = \frac{D - d - 4r_1}{2\cos\alpha} \tag{A.89}$$

$$g_4(X) = D_{r_{UL}} - D_r \geq 0 \tag{A.90}$$

$$g_5(X) = Z - \frac{\pi\,(d + 2r_1 + D_r\cos\alpha)}{D_{r_{UL}}\cos\alpha} \geq 0 \tag{A.91}$$

$$g_6(X) = \frac{\pi\,(D - 2r_1 - D_r\cos\alpha)}{D_{r_{LL}}\cos\alpha} - Z \geq 0 \tag{A.92}$$

$$g_7(X) = l_e - \frac{D_{r_{LL}}}{\chi} \geq 0 \tag{A.93}$$

$$g_8(X) = \frac{B - 2D_r\sin\alpha}{2\cos\alpha} - l_e \geq 0 \tag{A.94}$$

$$g_9(X) = D_r - K_{D\min}\frac{D - d - 4r_1}{2\cos\alpha} \geq 0 \tag{A.95}$$

$$g_{10}(X) = K_{D\max}\frac{D - d - 4r_1}{2\cos\alpha} - D_r \geq 0 \tag{A.96}$$

$$g_{11}(X) = (D_m\tan\alpha - l_e\cos\alpha - D_r\sin\alpha) \geq 0 \tag{A.97}$$

$$g_{12}(X) = (D - D_m - D_r\cos\alpha) - \varepsilon D_r \geq 0 \tag{A.98}$$

$$g_{13}(X) = 2\pi - 2Z\tan^{-1}\left(\frac{D_r}{D_m}\right) \geq \frac{Z\pi}{180} \tag{A.99}$$

$$g_{14}(X) = \frac{2D_m - (d + D)}{\cos\alpha} \geq 0 \tag{A.100}$$

$$g_{15}(X) = \frac{\frac{2}{1-\gamma} - D_r\left(\frac{1}{R} - \frac{1}{r_i}\right)}{\frac{2}{1-\gamma} + D_r\left(\frac{1}{R} - \frac{1}{r_i}\right)} \prec 1;$$

$$g_{16}(X) = \frac{\frac{2}{1+\gamma} - D_r\left(\frac{1}{R} - \frac{1}{r_o}\right)}{\frac{2}{1+\gamma} + D_r\left(\frac{1}{R} - \frac{1}{r_o}\right)} \prec 1 \tag{A.101}$$

$$g_{17}(X) = \frac{\frac{2}{1-\gamma} - D_r\left(\frac{1}{R} - \frac{1}{r_i}\right)}{\frac{2}{1-\gamma} + D_r\left(\frac{1}{R} - \frac{1}{r_i}\right)} \succ 0;$$

$$g_{18}(X) = \frac{\frac{2}{1+\gamma} - D_r\left(\frac{1}{R} - \frac{1}{r_o}\right)}{\frac{2}{1+\gamma} + D_r\left(\frac{1}{R} - \frac{1}{r_o}\right)} \succ 0 \tag{A.102}$$

Curvature radii of inner and outer raceways are given by,

$$r_i = 0.5\left(\frac{D_m}{\cos\alpha} - D_r\right); \quad r_o = 0.5\left(\frac{D_m}{\cos\alpha} + D_r\right) \tag{A.103}$$

$$g_{19}(X) = \left\{\left(\frac{D_r\cos\alpha + D_m}{2\cos\alpha} - R\,(1 - \cos\theta)\right)\cos\alpha + \frac{l_t}{2}\sin\alpha\right\} \succ \varpi \tag{A.104}$$

Here,

$$l_t = l_e + 2r_c \tag{A.105}$$

Roller semi-angle (θ) is given by,

$$\theta = \sin^{-1}\left(\frac{0.5l_e}{R}\right) \tag{A.106}$$

where, roller curvature radius (R) = 0.97

$$g_{20}(X) = 0.5B - \left\{\left(\frac{D_r\cos\alpha + D_m}{2\cos\alpha} - R\,(1 - \cos\theta)\right)\sin\alpha + \frac{l_t}{2}\cos\alpha\right\} \succ 0 \tag{A.107}$$

$$g_{21}(X) = \left\{\left(\frac{D_m - D_r\cos\alpha}{2\cos\alpha} + R\,(1 - \cos\theta)\right)\sin\alpha - \frac{l_t}{2}\cos\alpha\right\} \succ 0 \tag{A.108}$$

$$g_{22}(X) = [2\,(r_o - 0.5D_r)\cos\alpha] \succ D_m \tag{A.109}$$

6. Plate fin heat exchanger

Design variables,

$$\{X\} = [L_h,\, L_c, H,\, n,\, t,\, l,\, N_h] \tag{A.110}$$

Objective function:

$$\mathrm{Ns} = (1 - \varepsilon)\left[\frac{(\mathrm{T_{ci}} - \mathrm{T_{hi}})^2}{\mathrm{T_{ci}T_{hi}}}\right] + \left(\frac{\mathrm{Rcte_h}}{\mathrm{C_{ph}}}\right)\left(\frac{\Delta\mathrm{P_h}}{\mathrm{P_{hi}}}\right) + \left(\frac{\mathrm{Rcte_c}}{\mathrm{C_{pc}}}\right)\left(\frac{\Delta\mathrm{P_c}}{\mathrm{P_{ci}}}\right) \tag{A.111}$$

Design constraints:

$$C_1 = (\Delta\mathrm{P_h}/P_{\mathrm{hi}}) < 1; \quad C_2 = (\Delta\mathrm{P_c}/P_{\mathrm{ci}}) < 1; \quad C_3 = (1 - \varepsilon) < 1; \tag{A.112}$$

$$C_4 = Re_{\mathrm{h}} > 120; \quad C_5 = \alpha_{\mathrm{h}} > 0.134; \quad C_6 = \delta_{\mathrm{h}} > 0.012; \tag{A.113}$$

$$C_7 = \gamma_{\mathrm{h}} > 0.041; \quad C_8 = Re_{\mathrm{h}} < 10\text{^}4; \quad C_9 = \alpha_{\mathrm{h}} < 0.997; \tag{A.114}$$

$$C_{10} = \delta_{\mathrm{h}} < 0.048; \quad C_{11} = \gamma_{\mathrm{h}} < 0.121; \quad C_{12} = Re_{\mathrm{c}} > 120; \tag{A.115}$$

$$C_{13} = \alpha_{\mathrm{c}} > 0.134; \quad C_{14} = \delta_{\mathrm{c}} > 0.012; \quad C_{15} = \gamma_{\mathrm{c}} > 0.041; \tag{A.116}$$

$$C_{16} = Re_{\mathrm{c}} < 10\text{^}4; \quad C_{17} = \alpha_{\mathrm{c}} < 0.997; \quad C_{18} = \delta_{\mathrm{c}} < 0.048; \tag{A.117}$$

$$C_{19} = \gamma_{\mathrm{c}} < 0.121; \quad C_{20} = \Delta\mathrm{P_h} \leq 9500; \quad C_{21} = \Delta\mathrm{P_c} \leq 800; \tag{A.118}$$

$$C_{22} = L_{\mathrm{noflow}} \leq 1;$$

$$\mathrm{Q} = \varepsilon\mathrm{C_{min}}\,(\mathrm{T_{hi}} - \mathrm{T_{ci}})\,; \quad \mathrm{C_1} = \dot{\mathrm{m}}_{\mathrm{h}}\mathrm{C_{ph}}; \quad \mathrm{C_2} = \dot{\mathrm{m}}_{\mathrm{c}}\mathrm{C_{pc}} \tag{A.119}$$

$$\mathrm{C_{min}} = \min(\mathrm{C_1}, \mathrm{C_2})\,; \quad \mathrm{C_{max}} = \max(\mathrm{C_1}, \mathrm{C_2}) \tag{A.120}$$

$$\varepsilon = 1 - \mathrm{e}^{\left(\left(\frac{1}{\mathrm{Cr}}\right)\mathrm{NTU}^{0.22}\left(\mathrm{e}^{\left(-\mathrm{Cr}\,\mathrm{NTU}^{0.78}\right)} - 1\right)\right)} \tag{A.121}$$

$$C_r = \frac{C_{min}}{C_{max}} \tag{A.122}$$

$$\frac{1}{NTU} = C_{min}\left(\frac{Aff_h}{j_h C_{ph}\, Pr_h^{-0.667}\, \dot{m}_h A_h} + \frac{Aff_c}{j_c C_{pc}\, Pr_c^{-0.667}\, \dot{m}_c A_c}\right) \tag{A.123}$$

$$Aff_h = (H_h - t_h)\,(1 - n_h t_h)\, L_c N_h \tag{A.124}$$

$$Aff_c = (H_c - t_c)\,(1 - n_c t_c)\, L_h N_c \tag{A.125}$$

$$A_h = L_h L_c N_h\,(1 + (2n_h\,(H_h - t_h))) \tag{A.126}$$

$$A_c = L_h L_c N_c\,(1 + (2n_c\,(H_c - t_c))) \tag{A.127}$$

$$A_{tot} = A_h + A_c \tag{A.128}$$

$$j = 0.6522\,(Re)^{-0.5403}\,(\alpha)^{-0.1541}\,(\delta)^{0.1499}\,(\gamma)^{-0.0677}\,[1 + 5.3\times 10^{-5}\,(Re)^{1.34}\,(\alpha)^{0.504}\,(\delta)^{0.456}\,(\gamma)^{-1.055}]^{0.1} \tag{A.129}$$

$$f = 9.6243\,(Re)^{-0.7422}\,(\alpha)^{-0.1856}\,(\delta)^{0.3053}\,(\gamma)^{-0.2659}\,[1 + 7.7\times 10^{-7}\,(Re)^{4.429}\,(\alpha)^{0.920}\,(\delta)^{3.767}\,(\gamma)^{0.236}]^{0.1} \tag{A.130}$$

$$\alpha = {}^{s}/_{(H-t)},\ \delta = ({}^{t}/_{l}),\ \gamma = ({}^{t}/_{s}),\ s = ({}^{1}/_{n}) - t, \tag{A.131}$$

$$Re = \frac{\dot{m}dh}{Aff\mu};\quad dh = \frac{4s\,(H-t)\,l}{2\,(sl + (H-t)\,l + t\,(H-t)) + ts} \tag{A.132}$$

$$\Delta P = \frac{2fL\left(\frac{\dot{m}}{Aff}\right)^2}{\rho dh};\quad h = jC_p\, Pr^{\left(\frac{-2}{3}\right)}\,\frac{\dot{m}}{Aff} \tag{A.133}$$

$$L_{no\ flow} = H - 2t_p + N_h\left(2H + 2t_p\right) \tag{A.134}$$

$$P_{ho} = P_{hi} - \Delta P_h;\quad P_{co} = P_{ci} - \Delta P_c \tag{A.135}$$

$$T_{ho} = T_{hi} - \left(\varepsilon\frac{C_{min}}{C_{max}}\,(T_{hi} - T_{ci})\right) \tag{A.136}$$

$$T_{co} = T_{ci} - \left(\varepsilon\frac{C_{min}}{C_{max}}\,(T_{hi} - T_{ci})\right) \tag{A.137}$$

$$Ns = (1-\varepsilon)\left[\frac{(T_{ci} - T_{hi})^2}{T_{ci}T_{hi}}\right] + \left(\frac{Rcte_h}{C_{ph}}\right)\left(\frac{\Delta P_h}{P_{hi}}\right) + \left(\frac{Rcte_c}{C_{pc}}\right)\left(\frac{\Delta P_c}{P_{ci}}\right) \tag{A.138}$$

$$t_p = 0.005\ m \tag{A.139}$$

For hot fluid :

$$\dot{m} = 25.4\ kg/s,\ T_i = 460\ ^\circ C,\ P_i = 100\ kPa,\ Cp = 1060\ J/kg\ K, \tag{A.140}$$

$$\rho = 0.54\ kg/m^3,\ \mu = 0.000032\ N\ s/m^2,\ P_r = 0.69 \tag{A.141}$$

For cold fluid :

$$\dot{m} = 25\ kg/s,\ T_i = 300\ ^\circ C,\ P_i = 900\ kPa,\ Cp = 1060\ J/kg\ K, \tag{A.142}$$

$$\rho = 4.86\ kg/m^3,\ \mu = 0.000032\ N\ s/m^2,\ P_r = 0.69 \tag{A.143}$$

7. Shell and tube heat exchanger

Design variables, $\{X\} = [d_o, D_s, B]$ (A.144)

Objective function: $Ctot = Ci + Cod$ (A.145)

Design constraints:

$$C_1 = (L/D_s) \geq 3;\quad C_2 = (L/D_s) \leq 5 \tag{A.146}$$

$$C_3 = v_t \geq 1\ m/s;\quad C_4 = v_t \leq 2\ m/s \tag{A.147}$$

$$C_5 = v_s \geq 0.3\ m/s;\quad C_6 = v_s \leq 1\ m/s$$

$$C_7 = \Delta P_t \leq 35000\ Pa;\quad C_8 = \Delta P_s \leq 35000\ Pa$$

$$h_t = \begin{cases} \left(\frac{k_t}{d_i}\right)\left[3.657 + \frac{0.0677\left(Re_t\, Pr_t\left(\frac{d_i}{L}\right)\right)^{1.33}}{1+0.1\, Pr_t\left(Re_t\left(\frac{d_i}{L}\right)\right)^{0.3}}\right], Re_t \leq 2100 \\ \left(\frac{k_t}{d_i}\right)\left[\frac{\frac{f_t}{2}(Re_t - 1000)\, Pr_t}{1+12.7\sqrt{\frac{f_t}{2}}\left(Pr_t^{0.66} - 1\right)}\right], 2100 < Re_t < 10000 \\ 0.027\left(\frac{k_t}{d_i}\right) Re_t^{0.8}\, Pr_t^{0.33}\left(\frac{\mu_t}{\mu_{wt}}\right)^{0.14}, Re_t \geq 10000 \end{cases} \tag{A.148}$$

$$f_t = \begin{cases} (1.82\log(Re_t) - 1.64)^{-2}, Re_t \leq 2100 \\ 0.0054 + 0.000000023\left(Re_t^{3/2}\right), 2100 < Re_t < 4000 \\ 0.00128 + 0.1143\left(Re_t^{-1/3.214}\right), Re_t \geq 4000 \end{cases} \tag{A.149}$$

$$f_s = 1.44 Re_s^{(-0.15)};\quad h_s = 0.36\left(\frac{k_s}{de}\right) Re_s^{0.55} Pr_s^{0.33}\left(\frac{\mu_s}{\mu_{ws}}\right)^{0.14} \tag{A.150}$$

$$de = \frac{1.11}{d_o}\left(St^2 - 0.917 d_o^2\right);\quad St = 1.25 d_o;\quad Re_t = \frac{\rho_t v_t d_i}{\mu_t} \tag{A.151}$$

$$Re_s = \frac{\dot{m}_s d_e}{A_s \mu_s};\quad Nu_t = \frac{h_t d_i}{k_t};\quad Nu_s = \frac{h_s de}{k_s} \tag{A.152}$$

$$v_t = \frac{\dot{m}_t}{\left(\frac{\pi}{4}\right) d_i^2 \rho_t}\left(\frac{n}{Nt}\right);\quad v_s = \frac{\dot{m}_s}{\rho_s A_s};\quad d_i = 0.8 d_o \tag{A.153}$$

$$Nt = K_1\left(\frac{D_s}{d_o}\right)^{n_1};\quad A_s = D_s B\left(1 - \frac{d_o}{St}\right) \tag{A.154}$$

$$Pr_t = \frac{\mu_t Cp_t}{k_t};\quad Pr_s = \frac{\mu_s Cp_s}{k_s} \tag{A.155}$$

$$U = \frac{1}{\frac{1}{h_s} + Rf_s + \left(\frac{d_o}{d_i}\right)\left(Rf_t + \frac{1}{h_t}\right)} \tag{A.156}$$

$$\Delta T_{LM} = \frac{(T_{hi} - T_{co})\,(T_{ho} - T_{ci})}{\log_e\left(\frac{T_{hi}-T_{co}}{T_{ho}-T_{ci}}\right)} \tag{A.157}$$

$$F = \frac{\sqrt{R^2+1}}{R-1}\frac{\log_e\left(\frac{1-P}{1-PR}\right)}{\log_e\left(\frac{2-P\left(R+1-\sqrt{R^2+1}\right)}{2-P\left(R+1+\sqrt{R^2+1}\right)}\right)} \tag{A.158}$$

$$R = \frac{T_{hi} - T_{ho}}{T_{co} - T_{ci}};\ P = \frac{T_{co} - T_{ci}}{T_{hi} - T_{ci}};\quad A = \frac{Q}{UF\Delta T_{LM}} \tag{A.159}$$

$$Q = \dot{m}_h Cp_h\,(T_{co} - T_{ci});\quad L = \frac{A}{\pi d_o N t} \tag{A.160}$$

$$Ctot = Ci + Cod \tag{A.161}$$

$$Ci = 8000 + 259.2\ A^{0.91} \tag{A.162}$$

$$Cod = \sum_{j=1}^{ny} \frac{Co}{(1+i)^j} \tag{A.163}$$

$$Co = P_p CeH \tag{A.164}$$

$$P_p = \frac{1}{\eta}\left(\frac{\dot{m}_t}{\rho_t}\Delta P_t + \frac{\dot{m}_s}{\rho_s}\Delta P_s\right) \tag{A.165}$$

$$\Delta P_s = 1.44 Re_s^{-0.15}\left[\left(\frac{\rho_s v_s^2}{2}\right)\left(\frac{L}{B}\right)\left(\frac{D_s}{de}\right)\right] \tag{A.166}$$

$$\Delta P_t = \frac{\rho_t v_t^2}{2}\left(\frac{L}{d_i} f_t + 4\right) n \tag{A.167}$$

$K_1 = 0.249$, $n_1 = 2.207$, ny = 10 years, Ce = 0.00012 €/kWh, (A.168)

H = 7000 h/yr, i = 0.1 and $\eta = 0.8$. (A.169)

For shell side :

$\dot{m} = 22.07$ kg/s, $T_i = 33.9$ °C, $T_o = 29.4$ °C,
$\rho = 995$ kg/m^3, $Cp = 4.18$ kJ/kg K (A.170)

$\mu = 0.0008$ Pa s, $\mu_w = 0.00038$ Pa s, $k = 0.62$ W/m K,
$Rf = 0.00017$ m^{2}k/W (A.171)

For tube side:

$\dot{m} = 35.31$ kg/s, $T_i = 23.9$ °C, $T_o = 26.7$ °C,
$\rho = 995$ kg/m^3, $Cp = 4.18$ kJ/kg K (A.172)

$\mu = 0.00092$ Pa s, $\mu_w = 0.00052$ Pa s, $k = 0.62$ W/m K,
$Rf = 0.00017$ m^{2}k/W (A.173)

8. Welded beam

Design variables, $\{x\} = [x_1, x_2, h, b, t, l]$ (A.174)

Objective function: $f(x) = (1 + c_1)(x_1 t + l)h^2 + c_2 tb(l + L)$ (A.175)

Design constraints:

$$C_1(x) = \sigma(x) - S \le 0;\quad C_2(x) = F - P(x) \le 0 \tag{A.176}$$

$$C_3(x) = \delta(x) - \delta_{max} \le 0;\quad C_4(x) = \tau(x) - 0.577S \le 0 \tag{A.177}$$

$$x_1 \in \{0, 1\};\ x_2 \in \{0, 1, 2, 3\} \tag{A.178}$$

$$h = b = [0.06225, 2.0]\ \text{in},\ t = [2.0, 20.0]\ \text{in},\ b = [1.0, 10.0]\ \text{in} \tag{A.179}$$

$$\sigma(x) = \frac{6FL}{bt^2};\ \delta(x) = \frac{4FL^3}{Ebt^3} \tag{A.180}$$

$$P(x) = \frac{4.013bt^3\sqrt{EG}}{6L^2}\left[1 - \frac{t}{4L}\sqrt{\frac{E}{G}}\right] \tag{A.181}$$

$$\tau(x) = \sqrt{(\tau')^2 + (\tau'')^2 + 2\tau'\tau''\cos\theta} \tag{A.182}$$

$$\tau' = \frac{F}{A};\quad \tau'' = \frac{F\left(L + \frac{l}{2}\right)R}{J} \tag{A.183}$$

$$x_1 = 0:\begin{cases} \frac{A=\sqrt{2}hl}{j=\sqrt{2}hl\left[\frac{(h+t)^2}{4}+\frac{l^2}{12}\right]} \\ R = \frac{1}{2}\sqrt{l^2 + (h+t)^2} \\ \cos\theta = \frac{l}{2R} \end{cases};\quad x_2 = 1, 2, 3 \tag{A.184}$$

$$x_1 = 0:\begin{cases} \frac{A=\sqrt{2}h(t+l)}{j=\sqrt{2}hl\left[\frac{(h+t)^2}{4}+\frac{l^2}{12}\right]+\sqrt{2}hl\left[\frac{(h+l)^2}{4}+\frac{t^2}{12}\right]} \\ R = max\left\{\frac{1}{2}\sqrt{l^2 + (h+t)^2},\ \frac{1}{2}\sqrt{t^2 + (h+l)^2},\right\} \\ \cos\theta = \begin{cases} \frac{l}{2R},\ if\ l < t \\ \frac{t}{2R},\ otherwise \end{cases} \end{cases};\quad x_2 = 1, 2, 3 \tag{A.185}$$

9. belt–pulley drive

Design variables, $\{x\} = [d_1, d_2, b]$ (A.186)

Objective function: $f(x) = \pi\rho b\left[d_1 t_1 + d_2 t_2 + d_1^1 t_1^1 + d_2^1 t_2^1\right]$ (A.187)

Design constraints:

$$P = \frac{(T_1 - T_2)}{75}V;\ P = T_1\left(1 - \frac{T_2}{T_1}\right)\frac{\pi d_p N_p}{75 \times 60 \times 100}; \tag{A.188}$$

Here

$$\frac{T_2}{T_1} = 0.5,\ P = 10HP \tag{A.189}$$

$$T_1 = \frac{2864789}{d_p N_p};\ d_2 N_2 \le d_1 N_1;\ T_1 < \sigma_b b t_b \tag{A.190}$$

$$\sigma_b b t_b \ge \frac{2864789}{d_2 N_2}\ \text{Here},\ \sigma_b = 30\ \text{kg/cm}^2,$$

$$t_b = 1 \text{ cm}, N_2 = 250 \text{ rpm} \tag{A.191}$$

$$C_1(x) = b \geq \frac{381.97}{d_2}; \tag{A.192}$$

$$C_2(x) = b \leq 0.25 d_1 \tag{A.193}$$

$$t_1 = 0.1d_1, t_2 = 0.1d_2, t_1^1 = 0.1d_1^1, t_2^1 = 0.1d_2^1, \tag{A.194}$$

$$N_1 = 1000, N_2 = 250, N_1^1 = 500, N_2^1 = 500, \rho = 7.2 \times 10^{-3} \text{ kg/cm}^3 \tag{A.195}$$

$$15 \leq d_1 \leq 25; 70 \leq d_2 \leq 80; 4 \leq b \leq 10 \tag{A.196}$$

10. Hollow shaft

Design variables, $\{x\} = [d_0, k]$ (A.197)

Objective function: $f(x) = \frac{\pi}{4}\left(d_o^2 - d_i^2\right) L\rho$ (A.198)

Here,

$$k = \frac{d_i}{d_o} \tag{A.199}$$

Design constraints:

$$C_1(x) = \theta \geq \frac{TL}{GJ} \tag{A.200}$$

$$C_2(x) = T_{cr} \geq \frac{\pi d_o^3 E (1-k)^{2.5}}{12\sqrt{2}\left(1-\gamma^2\right)^{0.75}} \tag{A.201}$$

$$\theta = \frac{2\pi}{180}\frac{\text{rad}}{\text{m}}, T = 1 \times 10^5 \text{ kg cm}, G = 0.84 \times 10^6 \frac{\text{kg}}{\text{cm}^2}, \tag{A.202}$$

$$J = \frac{\pi}{32} d_o^4 (1 - k^4), T_{cr} = 1 \times 10^5 \text{ kg cm}, \gamma = 0.3, \tag{A.203}$$

$$E = 2.1 \times 10^6 \text{ kg/cm}^2 \tag{A.204}$$

$$7 \leq d_0 \leq 25, 0.7 \leq k \leq 0.97 \tag{A.205}$$

References

[1] A. Baykasoğlu, F.B. Ozsoydan, Adaptive firefly algorithm with chaos for mechanical design optimization problems, Appl. Soft Comput. 36 (2015) 152–164, http://dx.doi.org/10.1016/j.asoc.2015.06.056.

[2] Z. Cao, J. Xia, M. Zhang, J. Jin, L. Deng, X. Wang, J. Qu, Optimization of gear blank preforms based on a new R-GPLVM model utilizing GA-ELM, Knowl.-Based Syst. 83 (2015) 66–80, http://dx.doi.org/10.1016/j.knosys.2015.03.010.

[3] S. Panda, S.N. Panda, P. Nanda, D. Mishra, Comparative study on optimum design of rolling element bearing, Tribol. Int. 92 (2015) 595–604, http://dx.doi.org/10.1016/j.triboint.2015.07.034.

[4] J. Wang, S. Luo, D. Su, Multi-objective optimal design of cycloid speed reducer based on genetic algorithm, Mech. Mach. Theory 102 (2016) 135–148, http://dx.doi.org/10.1016/j.mechmachtheory.2016.04.007.

[5] S.-W. Kim, K. Kang, K. Yoon, D.-H. Choi, Design optimization of an angular contact ball bearing for the main shaft of a grinder, Mech. Mach. Theory 104 (2016) 287–302, http://dx.doi.org/10.1016/j.mechmachtheory.2016.06.006.

[6] A.B. Shinde, P.M. Pawar, Multi-objective optimization of surface textured journal bearing by Taguchi based grey relational analysis, Tribol. Int. 114 (2017) 349–357, http://dx.doi.org/10.1016/j.triboint.2017.04.041.

[7] H. Ding, J. Tang, Six sigma robust multi-objective optimization modification of machine-tool settings for hypoid gears by considering both geometric and physical performances, Appl. Soft Comput. 70 (2018) 550–561, http://dx.doi.org/10.1016/j.asoc.2018.05.047.

[8] D. Grooper, T.J. Harvey, L. Wang, Numerical analysis and optimization of surface textures for a tilting pad thrust bearing, Tribol. Int. 124 (2018) 134–144, http://dx.doi.org/10.1016/j.triboint.2018.03.034.

[9] J. Zhang, X, Qin, C. Xie, H. Chen, L. Jin, Optimization design on dynamic load sharing performance for an in-wheel motor speed reducer based on genetic algorithm, Mech. Mach. Theory 122 (2018) 132–147, http://dx.doi.org/10.1016/j.mechmachtheory.2017.12.016.

[10] P. Rai, A. Agrawal, M.L. Saini, C. Jodder, A.G. Barman, Volume optimization of helical gear with profile shift using real coded genetic algorithm, Procedia Comput. Sci. 133 (2018) 718–724, http://dx.doi.org/10.1016/j.procs.2018.07.127.

[11] D. Miler, D. Zezelj, A. Loncar, K. Vuckovic, Multi-objective spur gear pair optimization focused on volume and efficiency, Mech. Mach. Theory 125 (2018) 185–195, http://dx.doi.org/10.1016/j.mechmachtheory.2018.03.012.

[12] A. Robison, A. Vacca, Multi-objective optimization of circular-toothed gerotors for kinematics and wear by genetic algorithm, Mech. Mach. Theory 128 (2018) 150–168, http://dx.doi.org/10.1016/j.mechmachtheory.2018.05.011.

[13] A. Alessio, A methodology for simulation-based multiobjective gear design optimization, Mech. Mach. Theory 133 (2019) 95–111, http://dx.doi.org/10.1016/j.mechmachtheory.2018.11.013.

[14] X. Tian, J. Li, A novel improved fruit fly optimization algorithm for aerodynamic shape design optimization, Knowl.-Based Syst. 179 (2019) 77–91, http://dx.doi.org/10.1016/j.knosys.2019.05.005.

[15] W. Hou, X. Xu, X. Han, H. Wang, L. Tong, Multi-objective and multi-constraint design optimization for hat-shaped composite T-joints in automobiles, Thin-Walled Struct. 143 (2019) 106232, http://dx.doi.org/10.1016/j.tws.2019.106232.

[16] Y. Zhang, Z. Jin, Y.Chen, Hybrid teaching–learning-based optimization and neural network algorithm for engineering design optimization problems, Knowl.-Based Syst. (2019) in press. http://dx.doi.org/10.1016/j.knosys.2019.07.007.

[17] Y. Cheng, Z. Wang, W. Zhang, G. Haung, Particle swarm optimization algorithm to solve the deconvolution problem for rolling element bearing fault diagnosis, ISA Trans. 90 (2019) 244–267, http://dx.doi.org/10.1016/j.isatra.2019.01.012.

[18] A. Jat, R. Tiwari, Multi-objective optimization of spherical roller bearings based on fatigue and wear using evolutionary algorithm, J. King Saud Univ., Eng. Sci. 32 (1) (2020) 58–68, http://dx.doi.org/10.1016/j.jksues.2018.03.002.

[19] R.V. Rao, Rao algorithms: Three metaphor-less simple algorithms for solving optimization problems, Int. J. Ind. Eng. Comput. 11 (2020) 107–130, http://dx.doi.org/10.5267/j.ijiec.2019.6.002.

[20] L. Wang, Z. Wang, H. Liang, C. Huang, Parameter estimation of photovoltaic cell model with Rao-1 algorithm, Optik (2019) 163846, http://dx.doi.org/10.1016/j.ijleo.2019.163846.

[21] R.V. Rao, V.J. Savsani, D.P. Vakharia, Teaching-learning-based optimization: a novel method for constrained mechanical design optimization problems, Comput. Aided Des. 43 (3) (2011) 303–315, http://dx.doi.org/10.1016/j.cad.2010.12.015.

[22] R.V. Rao, Jaya: A simple and new optimization algorithm for solving constrained and unconstrained optimization problems, Int. J. Ind. Eng. Comput. 7 (1) (2016) 19–34, http://dx.doi.org/10.5267/j.ijiec.2015.8.004.

[23] R.V. Rao, Jaya: An Advanced Optimization Algorithm and its Engineering Applications, Springer International Publishing, 2019, http://dx.doi.org/10.1007/978-3-319-78922-4.

[24] R.V. Rao, G.G. Waghmare, A new optimization algorithm for solving complex constrained design optimization problems, Eng. Optim. 49 (1) (2016) 60–83, http://dx.doi.org/10.1080/0305215X.2016.1164855.

[25] K. Deb, M. Goyal, Optimizing engineering designs using a combined genetic search, in: I.T. Back (Ed.), 7th International Conference on Genetic Algorithms, 1997, pp. 512–28.

[26] S. He, E. Prempain, Q.H. Wu, An improved particle swarm optimizer for mechanical design optimization problems, Eng. Optim. 36 (5) (2004) 585–605, http://dx.doi.org/10.1080/03052150410001704854.

[27] E. Sandgren, Nonlinear integer and discrete programming in mechanical design optimization, J. Mech. Des. 112 (2) (1990) 223–229.

[28] A.H. Gandomi, X.-S. Yang, A.H. Alavi, Mixed variable structural optimization using Firefly algorithm, Comput. Struct. 89 (2011) 2325–2336, http://dx.doi.org/10.1016/j.compstruc.2011.08.002.

[29] C.X. Guo, J.S. Hu, B. Ye, Y.J. Cao, Swarm intelligence for mixed-variable design optimization, J. Zhejiang Univ. Sci. 5 (7) (2004) 851–860.

[30] K. Deb, A. Srinivasan, Innovization: Innovative Design Principles Through Optimization, Kanpur Genetic Algorithms Laboratory (Kangal), KanGAL Report Number 2005007, Indian Institute of Technology Kanpur, 2005.

[31] K.S. Kumar, R. Tiwari, R.S. Reddy, Development of an optimum design methodology of cylindrical roller bearings using genetic algorithms, Int. J. Comput. Methods Eng. Sci. Mech. 9 (6) (2008) 321–341, http://dx.doi.org/10.1080/15502280802362995.
[32] R.D. Dandagwhal, V.D. Kalyankar, Design optimization of rolling element bearings using advanced optimization technique, Arab. J. Sci. Eng. 44 (2019) 7407–7422, http://dx.doi.org/10.1007/s13369-019-03767-0.
[33] R.K. Shah, D.P. Sekulic, Fundamentals of Heat Exchanger Design, John Wiley & Sons Inc., Hoboken, USA, 2003.
[34] M. Yousefi, A.N. Darus, H. Mohammadi, Second law based optimization of plate fin heat exchanger using Imperialist Competitive Algorithm, Int. J. Phys. Sci. 6 (20) (2011) 4749–4759, http://dx.doi.org/10.5897/IJPS11.514.
[35] H. Zarea, F.M. Kashkooli, A.M. Mehryan, M.R. Saffarian, E.N. Beherghani, Optimal design of plate-fin heat exchangers by a Bees Algorithm, Appl. Therm. Eng. 69 (2014) 267–277.
[36] E.H.V. Segundo, V.C. Mariani, L.S. Coelho, Design of heat exchangers using falcon optimization algorithm, Appl. Therm. Eng. 156 (2019) 119–144.
[37] D.Q. Kern, Process Heat Transfer, McGraw-Hill, 1950.
[38] A.C. Caputo, P.M. Pelagagge, P. Salini, Heat exchanger design based on economic optimization, Appl. Therm. Eng. 27 (2007) 1151–1159.
[39] A.S. Sahin, B. Kilic, U. Kilic, Design and economic optimization of shell and tube heat exchangers using Artificial Bee Colony (ABC) algorithm, Energy Convers. Manage. 52 (2011) 3356–3362.
[40] V.K. Patel, R.V. Rao, Design optimization of shell and tube heat exchanger using particle swarm optimization technique, Appl. Therm. Eng. 30 (2010) 1417–1425.
[41] A. Hadidi, A. Nazari, Design and economic optimization of shell and tube heat exchangers using biogeography-based (BBO) algorithm, Appl. Therm. Eng. 51 (2013) 1263–1272.
[42] K. Deb, M. Goyal, A combined genetic adaptive search (GeneAS) for engineering design, Comput. Sci. Inform. 26 (1996) 30–45.
[43] J. Kennedy, R. Eberthart, A discrete binary version of the particle swarm optimizer, IEEE Conf. Comput. Cybern. Simul. 5 (1997) 4104–4108.
[44] D. Datta, J.R. Figueira, A real-integer-discrete-coded particle swarm optimization for design problems, Appl. Soft Comput. 11 (2011) 3625–3633, http://dx.doi.org/10.1016/j.asoc.2011.01.034.
[45] B. Thamaraikannan, V. Thirunavukkarasu, Design optimization of mechanical components using an enhanced teaching-learning based optimization algorithm with differential operator, Math. Probl. Eng. (2014) 309327, http://dx.doi.org/10.1155/2014/309327.
[46] R. Tiwari, V. Waghole, Optimization of spherical roller bearing design using artificial bee colony algorithm and grid search method, Int. J. Comput. Methods Eng. Sci. Mech. 16 (4) (2015) 221–233, http://dx.doi.org/10.1080/15502287.2015.1045998.